AD-A077 067 RENESSELAER POLYTECHNIC INST TROY NY DEPT OF MECHANI--ETC F/G 20/1
AN ANALYSIS OF TRANSVERSE MODES IN ACOUSTIC SURFACE WAVE RESONA--ETC(U)
SEP 79 B K SINHA , H F TIERSTEN N00014-76-C-0368
UNCLASSIFIED RPI-TR-29 NL

1 OF 1
AD-
A077067

END
DATE
FILMED
12-79
DDC

Rensselaer Polytechnic Institute
Troy, New York 12181

AN ANALYSIS OF TRANSVERSE MODES IN ACOUSTIC SURFACE WAVE RESONATORS

by

B.K. Sinha and H.F. Tiersten

Office of Naval Research
Contract N00014-76-C-0368
Project NR 318-009
Technical Report No. 29

September 1979

Rensselaer Polytechnic Institute

Troy, New York 12181

AN ANALYSIS OF TRANSVERSE MODES IN ACOUSTIC SURFACE WAVE RESONATORS

by

B.K. Sinha and H.F. Tiersten

Office of Naval Research
Contract N00014-76-C-0368
Project NR 318-009
Technical Report No. 29

September 1979

Unclassified

SECURITY CLASSIFICATION OF THIS PAGE (When Data Entered)

REPORT DOCUMENTATION PAGE

READ INSTRUCTIONS BEFORE COMPLETING FORM

1. REPORT NUMBER: No. 29

2. GOVT ACCESSION NO.

3. RECIPIENT'S CATALOG NUMBER

4. TITLE (and Subtitle): AN ANALYSIS OF TRANSVERSE MODES IN ACOUSTIC SURFACE WAVE RESONATORS.

5. TYPE OF REPORT & PERIOD COVERED: Technical Report

6. PERFORMING ORG. REPORT NUMBER

7. AUTHOR(s): B.K. Sinha and H.F. Tiersten

8. CONTRACT OR GRANT NUMBER(s): N00014-76-C-0368

9. PERFORMING ORGANIZATION NAME AND ADDRESS
Department of Mechanical Engineering,
Aeronautical Engineering & Mechanics
Rensselaer Polytechnic Institute
Troy, New York 12181

10. PROGRAM ELEMENT, PROJECT, TASK AREA & WORK UNIT NUMBERS: NR 318-009

11. CONTROLLING OFFICE NAME AND ADDRESS
Office of Naval Research
Physics Branch

12. REPORT DATE: September 1979

13. NUMBER OF PAGES: 50

14. MONITORING AGENCY NAME & ADDRESS (if different from Controlling Office)

15. SECURITY CLASS. (of this report): Unclassified

15a. DECLASSIFICATION/DOWNGRADING SCHEDULE

16. DISTRIBUTION STATEMENT (of this Report)

Distribution of this document is unlimited.

RPI-TR-29

17. DISTRIBUTION STATEMENT (of the abstract entered in Block 20, if different from Report)

18. SUPPLEMENTARY NOTES

19. KEY WORDS (Continue on reverse side if necessary and identify by block number)

Surface Waves	Reflecting Arrays	Bandpass Filters
Piezoelectricity	Transverse Modes	
Elasticity	Guided Surface Waves	
Surface Wave Reflectors	Reflecting Strips	
Surface Wave Resonators	Surface Wave Filters	

20. ABSTRACT (Continue on reverse side if necessary and identify by block number)

A system of approximate surface wave equations employed in an earlier treatment of the reflection of straight-crested surface waves by arrays of reflecting strips is extended to the case of variable-crested surface waves. Although the basic straight-crested surface wave velocities are determined as in the previous treatment, in the present case a reduction in straight-crested surface wave velocity in the unplated region due to the adjacent plated regions, which is essential for the existence of the guided transverse modes, is determined by means of a perturbation procedure.

DD FORM 1 JAN 73 1473 EDITION OF 1 NOV 65 IS OBSOLETE
S/N 0102-014-6601

Unclassified

SECURITY CLASSIFICATION OF THIS PAGE (When Data Entered)

409359

The attendant depth dependence for each region is employed in the variational principle as in the earlier treatment, but now the variable cresting relation for the isotropic substrate is incorporated in the description. The resulting equations are applied in the determination of both the transverse modes in each region and the transmission line representation of each mode. The transverse wavenumbers in a given mode are taken to be the same in the plated and unplated regions in order that the interior edge conditions be satisfied pointwise. The system of parallel transmission lines is applied in the analysis of the reflection of variable-crested surface waves by uniformly spaced arrays. The response to a rectangular input of a particular reflecting array consisting of aluminum reflecting strips on ST-cut quartz is calculated and compared with measurements.

AN ANALYSIS OF TRANSVERSE MODES IN ACOUSTIC SURFACE WAVE RESONATORS

B.K. Sinha and H.F. Tiersten
Department of Mechanical Engineering,
Aeronautical Engineering & Mechanics
Rensselaer Polytechnic Institute
Troy, New York 12181

ABSTRACT

A system of approximate surface wave equations employed in an earlier treatment of the reflection of straight-crested surface waves by arrays of reflecting strips is extended to the case of variable-crested surface waves. Although the basic straight-crested surface wave velocities are determined as in the previous treatment, in the present case a reduction in straight-crested surface wave velocity in the unplated region due to the adjacent plated regions, which is essential for the existence of the guided transverse modes, is determined by means of a perturbation procedure. The attendant depth dependence for each region is employed in the variational principle as in the earlier treatment, but now the variable cresting relation for the isotropic substrate is incorporated in the description. The resulting equations are applied in the determination of both the transverse modes in each region and the transmission line representation of each mode. The transverse wavenumbers in a given mode are taken to be the same in the plated and unplated regions in order that the interior edge conditions be satisfied pointwise. The system of parallel transmission lines is applied in the analysis of the reflection of variable-crested surface waves by uniformly spaced arrays. The response to a rectangular input of a particular reflecting array consisting of aluminum reflecting strips on ST-cut quartz is calculated and compared with measurements.

1. Introduction

The reflection of surface waves in high Q acoustic surface wave resonators is achieved by employing periodic arrays of reflecting strips (or grooves) which reflect almost all of the energy in an incident surface wave as a surface wave, i.e., without much scattering into bulk waves, when the wavelength matches the spacing. Considerable work has been done[1-7] in the description of such device structures. In all of those treatments[1-6] model parameters are measured which are never related to the fundamental material constants. In an earlier work[7], a system of approximate one-dimensional surface wave equations and edge conditions in a single scalar variable was derived from the variational principle of linear piezoelectricity and applied in the analysis of the reflection of surface waves by arrays of reflecting strips. These approximate equations are expressed in terms of the known fundamental material constants and no measurement of model parameters is required. However, it should be noted that scattering into bulk waves has been ignored in all of the above-mentioned treatments[1-7]. This scattering has been included[8-10] in more fundamental studies of the reflection of surface waves from small surface impedance discontinuities, but this work cannot readily be extended to the treatment of the large number of discontinuities encountered in a reflective array as noted in Ref.7 along with the fact that certain results that could in principle be obtained from that work[8-10] could be of considerable value in extending the treatment presented here to include scattering loss.

In a previous paper it was pointed out[11] that surface waves encountering reflective arrays of strips are not straight-crested but are variable-crested on account of the finite width of the strips, which causes transverse modes to propagate in the array. However, all of the aforementioned

treatments[1-7] are for straight-crested surface waves only. Recently, some analytical work[12-14] has been done on transverse modes in acoustic surface wave reflecting arrays, all of which uses coupled mode scalar wave equations with model parameters that are measured and never related to the fundamental material constants.

In this paper the system of approximate surface wave equations employed in the earlier treatment[7] of the reflection of straight-crested surface waves by arrays of reflecting strips is extended to the case of variable-crested surface waves. As in the straight-crested case these equations are expressed in terms of the fundamental material constants and no measurement of model parameters is required. Although the basic straight-crested surface wave velocities are determined as in the previous treatment[7], in the present case a reduction in straight-crested surface wave velocity in the unplated region due to the adjacent plated regions, which is essential for the existence of the guided transverse modes, is determined by means of a perturbation procedure. At the same time an increase in the straight-crested surface wave velocity in the plated region due to the adjacent unplated region is found. The attendant depth dependence for each region is employed in the variational principle as in the earlier treatment, but now the variable cresting relation for an isotropic substrate[15,16] is incorporated in the description. This isotropic approximation for the variable cresting is employed because variable-crested surface wave solutions of the three-dimensional equations for anisotropic materials have not been determined. This approximation is deemed not to have an appreciable effect on a calculation primarily because the essential anisotropy is still retained in the equations. The resulting equations are applied in the determination of both the transverse modes in each region and the transmission line representation of each mode. The

transverse wave numbers in a given mode are taken to be the same in the plated and unplated regions in order that the interior edge conditions be satisfied pointwise. The system of parallel transmission lines is applied in the analysis of the reflection of variable-crested surface waves by uniformly spaced arrays. The response to a rectangular input of a particular reflecting array consisting of aluminum reflecting strips on ST-cut quartz is calculated. The calculations clearly reveal the existence of resonance peaks on the high frequency side of the fundamental resonance, as observed by Staples and Smythe[17]. The calculated spacing of the peaks is in reasonably good agreement with the measured values. We believe the agreement would be improved if a more accurate dispersion curve for the aluminum film on the quartz substrate were employed because the wavelengths used in the experiments were a little too short for the thin film approximation[15,18] employed in the calculations. In addition, for a given reflection coefficient we find that the number of reflecting strips for the fundamental variable-crested mode is larger than we found earlier in the straight-crested case. This is essentially a result of the newly defined velocities in each region, which are required for the energy to be confined. Furthermore, on account of certain observations recently made[19], we show that although the amplitude of the fundamental transverse mode has an inflection point at the edge of the strip, the power has an inflection point well inside the edge of the strip.

2. Straight-Crested Surface Waves

Solutions satisfying the differential equations and boundary conditions of linear piezoelectricity for straight-crested acoustic surface waves may be written in the form

$$u_j = \sum_{m=1}^{4} C^{(m)} A_j^{(m)} e^{i\beta_m \xi x_2} e^{i\xi(x_1 - \omega t)},$$

$$\varphi = \sum_{m=1}^{4} C^{(m)} A_4^{(m)} e^{i\beta_m \xi x_2} e^{i\xi(x_1 - \omega t)}, \qquad (2.1)$$

for propagation in the direction x_1, with x_2 normal to the surface. For a given set of boundary conditions values of $C^{(m)}$, $A_j^{(m)}$, $A_4^{(m)}$ and β_m are determined numerically. These calculations have been performed for thin aluminum films on ST-cut quartz[20], and the dispersion curves obtained are plotted in Fig.1. However, the resulting phase velocities are either for the completely free or completely plated substrate, and in the case of the reflecting array the substrate is only partially plated, as shown in Fig.2. Consequently, we must find the phase velocities in the unplated regions when the adjacent regions are plated and in the plated regions when the adjacent regions are unplated in order to obtain the approximate surface wave equations and edge conditions.

When the plating is nonconducting the mean phase velocity over a wavelength for a partially plated substrate may readily be determined by means of a perturbation procedure. We determine the mean velocity only at resonance, i.e., when the half wavelength equals the periodicity, because the result thus found will hold for all longer wavelengths and the nearby shorter ones of interest. It has been shown[20] that the reduction in mean surface wave velocity ΔV^m is given by

$$\Delta V^m = H_1 / 2V_1 \xi_1^2, \qquad (2.2)$$

where V_1 is the free unperturbed surface wave velocity and

$$H_1 = - \int_0^{2\pi/\xi_1} \left[T_{2j} g_j^1\right]_{x_2=0} dx_1 = -2\ell h' \xi^2 \left[\left(\frac{4\mu'(\lambda'+\mu')}{\lambda'+2\mu'} - \rho' V_1^2\right) g_1^1 g_1^{1*} - \right.$$

$$\left. - \rho' V_1^2 g_2^1 g_2^{1*} + (\mu' - \rho' V_1^2) g_3^1 g_3^{1*}\right], \qquad (2.3)$$

where T_{2j} is given in Eq. (4.1) of Ref. 20, ρ', λ' and μ' are the mass density and Lamé constants for the film material and the g_j^1 are the normalized mechanical displacement components for the surface wave eigensolution for the free substrate, which are defined by

$$g_j^1 = u_j / N_1 , \qquad (2.4)$$

where

$$N_1^2 = \frac{i\pi}{\xi^2} \rho \sum_{m=1}^{4} \sum_{n=1}^{4} \frac{C^{(m)} A_k^{(m)} C^{(n)*} A_k^{(n)*}}{(\beta_m - \beta_n^*)} , \qquad (2.5)$$

and * denotes complex conjugate. The foregoing equations clearly show that the reduction in mean surface wave velocity ΔV^m is directly proportional to 2ℓ, the portion of the surface plated in a wavelength. As shown in Ref. 20 if Eq. (2.2) is used iteratively, the resulting dispersion for the fully plated case can be obtained to any desired accuracy. Clearly, the same is true for the mean velocity in the partially plated case.

When the plating is conductive the foregoing determination of the mean velocity does not hold because the electrical boundary condition in the plated and unplated regions is different and this particular difference cannot conveniently be treated by means of a perturbation procedure because it requires a perturbation from one set of eigenconditions to another[20]. Under these circumstances the boundary conditions in the plated region are

$$T_{2j} = - \delta_{jb} 2h'\mu' \left[\left(\frac{3\lambda'+2\mu'}{\lambda'+2\mu'}\right) u_{a,ab} + u_{b,aa}\right] + 2h'\rho' \ddot{u}_j ,$$

$$\varphi = 0 , \quad \text{at } x_2 = 0 , \qquad (2.6)$$

where δ_{jb} is the Kronecker delta with the provision that b cannot take the value 2 and

$$T_{2j} = c^{E}_{2jk\ell} u_{k,\ell} + e_{k2j} \varphi_{,2} , \tag{2.7}$$

while the boundary conditions in the unplated region are

$$T_{2j} = 0 , \quad D_2 = -\epsilon_o \xi\varphi , \quad \text{at } x_2 = 0 , \tag{2.8}$$

where ϵ_o is the permittivity of free-space and

$$D_2 = e_{2k\ell} u_{k,\ell} - \epsilon^{S}_{2k} \varphi_{,k} . \tag{2.9}$$

The dispersion curve obtained from the solution satisfying (2.6) is plotted as the curve labeled $\bar{V}_o$ in Fig.1, while from the solution satisfying (2.8) we obtain the straight line labeled V_o in Fig.1. The mean phase velocity[21] $\hat{V}^m$ is now defined so that the time of travel over $(\ell + d)$ is equal to the time of travel of $\bar{V}_o$ over ℓ plus V_o over d and we write

$$\frac{\ell}{\bar{V}_o} + \frac{d}{V_o} = \frac{(\ell + d)}{\hat{V}^m} , \tag{2.10}$$

which determines $\hat{V}^m$ when the other quantities are known. Clearly, this definition can be used even when the plating is nonconductive, and consequently (2.10) can replace (2.2). It is easily verified that the two definitions are equivalent when V_o and $\bar{V}_o$ differ by a small amount, which is the case of interest here. For $\ell = d$, $\hat{V}^m$ is plotted in Fig.1.

From the mean surface wave velocity $\hat{V}^m$ in a wavelength[21], which we have determined, we must obtain the surface wave velocities V and $\bar{V}$, which are the phase velocity in the unplated regions when the adjacent regions are plated and the phase velocity in the plated region when the adjacent regions are unplated, respectively. One way of doing this is to equate the time average over a cycle of the kinetic energy of the solution with the mean velocity, which has been determined, with the time average over a cycle of the sum of

the kinetic energies in the unplated and plated regions, which have the unknown phase velocities V and $\bar{V}$. To this end we write

$$\frac{\rho}{2}\int_0^{\ell+d} dx_1 \int_0^{\infty} \dot{\hat{q}}_j \dot{\hat{q}}_j^* \, dx_2 + \frac{2h'\rho'}{2}\int_0^{\ell} \dot{\hat{q}}_j(0)\dot{\hat{q}}_j^*(0)\, dx_1 = \frac{\rho}{2}\int_0^{\ell} dx_1 \int_0^{\infty} \dot{\bar{q}}_j \dot{\bar{q}}_j^* \, dx_2$$
$$+ \frac{2h'\rho'}{2}\int_0^{\ell} \dot{\bar{q}}_j(0)\dot{\bar{q}}_j^*(0)\, dx_1 + \frac{\rho}{2}\int_{\ell}^{\ell+d} dx_1 \int_0^{\infty} \dot{q}_j \dot{q}_j^* \, dx_2 , \qquad (2.11)$$

where $\hat{q}_j$, $\bar{q}_j$ and q_j are the normalized eigensolutions for the mean velocity V^m in a wavelength, the velocity $\bar{V}$ in the plated region and the velocity V in the unplated region, respectively. The eigensolutions $\bar{q}_j$, q_j and $\hat{q}_j$ are normalized in such a way that

$$\bar{q}_j(0)\bar{q}_j^*(0) = q_j(0)q_j^*(0) = \hat{q}_j(0)\hat{q}_j^*(0) . \qquad (2.12)$$

For the same propagation wavenumber ξ, from (2.11), we obtain

$$\rho(\ell+d)(\hat{V}^m)^2 \int_0^{\infty} \hat{q}_j\hat{q}_j^* \, dx_2 + \rho' \ell 2h' (\hat{V}^m)^2 \hat{q}_j(0)\hat{q}_j^*(0) = \rho\ell\bar{V}^2 \int_0^{\infty} \bar{q}_j\bar{q}_j^* \, dx_2$$
$$+ \rho' \ell 2h' \bar{V}^2 \bar{q}_j(0)\bar{q}_j^*(0) + \rho d V^2 \int_0^{\infty} q_j q_j^* \, dx_2 . \qquad (2.13)$$

Since $\hat{V}^m$ is known, a corrected $\hat{q}_j$ is found by satisfying the differential equations and traction-free boundary conditions with the known $\hat{V}^m$ (the electric boundary condition is ignored), after which the left-hand side of (2.13) is known. From (2.13) we may write the two independent recursive equations

$$V_n^2 = \frac{(\hat{V}^m)^2}{\beta_{n-1}}\left[\frac{\ell+d}{d}\beta^m + \frac{\ell}{d}\frac{\rho'}{\rho} 2h'\hat{q}_j(0)\hat{q}_j^*(0)\right] - \frac{\bar{V}_{n-1}^2}{\beta_{n-1}}\frac{\ell}{d}\left[\bar{\beta}_{n-1}\right.$$
$$\left. + \frac{\rho'}{\rho} 2h'\bar{q}_j(0)\bar{q}_j^*(0)\right] , \qquad (2.14)$$

$$\bar{V}_n^2 = \frac{(\hat{V}^m)^2}{\bar{\beta}_{n-1}}\left[\frac{\ell+d}{\ell}\beta^m + \frac{\rho'}{\rho} 2h'\hat{q}_j(0)\hat{q}_j^*(0)\right] - \frac{d}{\ell+d}\frac{\beta_n}{\bar{\beta}_{n-1}} V_n^2 , \qquad (2.15)$$

where

$$\mathcal{P}^m = \int_0^\infty \hat{g}_j \hat{g}_j^* \, dx_2 , \quad \mathcal{P}_n = \int_0^\infty g_j g_j^* \, dx_2 , \quad \bar{\mathcal{P}}_n = \int_0^\infty \bar{g}_j \bar{g}_j^* \, dx_2 , \tag{2.16}$$

in which g_j and $\bar{g}_j$ are the normalized eigensolutions corresponding to the phase velocities V_n and $\bar{V}_n$ at any stage of the iteration. Equations (2.14) and (2.15) are solved by successive alternate iteration. In this process one starts with the free surface wave solution for g_j and the fully plated surface wave solution for $\bar{g}_j$ and the known respective velocities V_o and $\bar{V}_o$. Then Eq. (2.14) is solved for V_1 using $\bar{V}_o$ for $\bar{V}_{1-1}$, after which $\bar{V}_1$ is obtained from (2.15) using the V_1 just determined. Now the corrected g_j and $\bar{g}_j$ are determined from the differential equations in the manner set forth above using the present iterated velocities V_1 and $\bar{V}_1$. This process is continued until both V and $\bar{V}$ converge. Both V and $\bar{V}$ converge to better than 10 digit accuracy in about 15 iterations. For the case $\ell = d$, the corrected phase velocities V and $\bar{V}$ are plotted in Fig. 3 as the curves labeled 1 and 2, respectively.

3. Approximate Surface Wave Equations

In this section we derive the approximate two-dimensional surface wave equations and edge conditions in one scalar variable from the variational principle of linear piezoelectricity. It has been shown[16] that the variational principle of linear piezoelectricity for a partially plated substrate, shown in Fig. 4, may be written in the form

$$\int_0^\infty \int_A (\rho \ddot{u}_j \delta u_j + T_{\nu\ell} \delta u_{\ell,\nu} + T_{a\ell} \delta u_{\ell,a} + D_\nu \delta\varphi_{,\nu} + D_a \delta\varphi_{,a}) dA dx_\nu$$
$$+ \int_0^\infty \int_{\bar{A}} (\rho \ddot{\bar{u}}_j \delta\bar{u}_j + \bar{T}_{\nu\ell} \delta\bar{u}_{\ell,\nu} + \bar{T}_{a\ell} \delta\bar{u}_{\ell,a} + \bar{D}_\nu \delta\bar{\varphi}_{,\nu} + \bar{D}_a \delta\bar{\varphi}_{,a}) dA dx_\nu$$
$$+ \int_{\substack{\bar{A} \\ x_\nu = 0}} 2h' [\rho' \ddot{\bar{u}}_j \delta\bar{u}_j + \lambda'_o \bar{u}_{a,a} \delta\bar{u}_{b,b} + \mu' (\bar{u}_{a,b} + \bar{u}_{b,a}) \delta\bar{u}_{b,a}] dA$$

$$= \int_{\bar{A}} \epsilon_o \varphi^a_{,\nu} \delta\varphi \, dA + \int_o^\infty \oint_{\bar{C}} (t_k \delta u_k - \sigma \delta\varphi) \, ds \, dx_\nu$$

$$+ \int_o^\infty \oint_{\bar{C}} (\bar{t}_k \delta \bar{u}_k - \bar{\sigma} \delta\bar{\varphi}) ds dx_\nu + 2h' \oint_{\substack{\bar{C} \\ x_\nu = 0}} \bar{t}'_k \delta \bar{u}_k \, ds \, , \qquad (3.1)$$

where we have introduced the convention that a bar over a quantity indicates that the quantity is associated with the plated region, the primes refer to the plating material, the prescribed quantities in Eq. (3.1) are over the portions of the cylindrical boundary associated with the plated and unplated regions, respectively, and

$$\lambda'_o = 2\mu'\lambda'/(\lambda' + 2\mu') \qquad (3.2)$$

is the plate Lamé constant. In Eq. (3.1) we have employed Cartesian tensor notation, the summation convention for repeated tensor indices, the dot notation for differentiation with respect to time, and the convention that a comma followed by an index, say j, denotes differentiation with respect to the space coordinate x_j. In addition, we have introduced the further conventions, employed in Ref. 16, that repeated Greek indices are not to be summed and a and b can equal τ and σ but skip ν, which refers to the direction normal to the surface. The quantities T_{ij}, u_j, D_i, and t_k are the components of stress, mechanical displacement, electric displacement and surface traction, respectively; ρ, φ, σ, and φ^a are the mass density, electric potential, surface charge density, and free-space electric potential, respectively; and ϵ_o is the dielectric constant in the space outside the substrate. In addition to Eq. (3.1) we have the linear piezoelectric constitutive equations, which can be written in the form

$$T_{ij} = c^{E}_{ijk\ell} u_{k,\ell} + e_{kij}\varphi_{,k} ,$$

$$D_i = e_{ik\ell} u_{k,\ell} - \epsilon^{S}_{ik}\varphi_{,k} , \tag{3.3}$$

where $c^{E}_{ijk\ell}$, e_{kij}, and ϵ^{S}_{ik} are the elastic, piezoelectric, and dielectric constants, respectively.

As in Ref. 16, the basic assumption employed in obtaining the approximate two-dimensional surface-wave equations in one scalar variable from (3.1) is that the x_ν-dependence of the variables is to be obtained from the three-dimensional surface-wave solution functions in Eq. (2.21) of Ref. 16. In addition, certain shaping modifications are introduced, which are obtained from the variable-crested surface-wave solutions for isotropic substrates determined previously[15] from the three-dimensional elasticity equations. Accordingly, we write

$$u_j = \hat{\alpha}_j(x_\nu)\Psi(x_\tau, x_\sigma, t) , \quad \varphi = \hat{\alpha}_4(x_\nu)\Psi(x_\tau, x_\sigma, t) , \tag{3.4}$$

where Ψ is the scalar surface wave variable, and

$$\hat{\alpha}_j = \sum_{n=1}^{4} C^{(n)} A_j^{(n)} \exp(i\beta_{(n)}\xi x_\nu) ,$$

$$\hat{\alpha}_4 = \sum_{n=1}^{4} C^{(n)} A_4^{(n)} \exp(i\beta_{(n)}\xi x_\nu) , \tag{3.5}$$

for straight-crested surface waves. As in Ref. 16, for variable-crested surface waves the α_j and $\hat{\alpha}_4$ are changed in accordance with the variable-crested solution for the isotropic substrate, and in those portions of the straight-crested solution that are employed in the approximate (or exact) variable-crested solution, ξ in the straight-crested solution is to be replaced by ζ, where

$$\zeta^2 = \xi^2 + \kappa^2 , \tag{3.6}$$

and κ is the purely real part of the shaping wave number for trigonometric cresting or the purely imaginary part of the decay factor for exponential cresting. It has been shown[15] that this procedure converts the straight-crested surface-wave solutions to the variable-crested surface-wave solutions exactly in the isotropic case. Since variable-crested surface-wave solutions have not been obtained for anisotropic substrates, this result for the isotropic case is employed in the anisotropic case as an approximation. Essentially, this approximation assumes that, even in the anisotropic case, variable cresting is in accordance with known results for the isotropic case. Moreover, since in the anisotropic case at hand the u_σ (or Love type) displacement component exists in the x_τ propagating straight-crested surface wave in addition to the u_τ and u_ν (or Rayleigh type) displacement components, we must account for the variable cresting due to the Love type displacement in the straight-crested solution as well as the above-mentioned variable cresting resulting from the Rayleigh type displacements in the straight-crested solution. We naturally assume that the variable cresting resulting from the straight-crested Love type displacement component is in accordance with the known result for the isotropic case, as we already have for the Rayleigh type displacement components. It has been shown[16] that in this case to a good approximation the variable-crested solution can be written in the form

$$u_\tau = P\left[\hat{\alpha}_\tau(x_\nu) - \frac{i\kappa}{\xi}\hat{\alpha}_\sigma(x_\nu)\right] e^{i\kappa x_\sigma} e^{i\xi(x_\tau - Vt)},$$

$$u_\sigma = P\left[\hat{\alpha}_\sigma(x_\nu) - \frac{i\kappa}{\xi}\hat{\alpha}_\tau(x_\nu)\right] e^{i\kappa x_\sigma} e^{i\xi(x_\tau - Vt)},$$

$$u_\nu = P\frac{\zeta}{\xi}\hat{\alpha}_\nu(x_\nu) e^{i\kappa x_\sigma} e^{i\xi(x_\tau - Vt)}, \quad \varphi = P\hat{\alpha}_4(x_\nu) e^{i\kappa x_\sigma} e^{i\xi(x_\tau - Vt)}, \qquad (3.7)$$

where the $\hat{\alpha}_j$ and $\hat{\alpha}_4$ are given in (3.5) with ξ appropriately replaced by the resultant wavenumber ζ in accordance with the earlier discussion. Clearly, if we define α_j and α_4 by

$$\alpha_\tau(x_\nu) = \hat{\alpha}_\tau(x_\nu) - \frac{i\kappa}{\xi}\hat{\alpha}_\sigma(x_\nu), \quad \alpha_\nu(x_\nu) = \frac{\zeta}{\xi}\hat{\alpha}_\nu(x_\nu),$$

$$\alpha_\sigma(x_\nu) = \hat{\alpha}_\sigma(x_\nu) - \frac{i\kappa}{\xi}\hat{\alpha}_\tau(x_\nu), \quad \alpha_4(x_\nu) = \hat{\alpha}_4(x_\nu), \tag{3.8}$$

we may write (3.4) in the form

$$u_j = \alpha_j(x_\nu)\psi(x_\tau, x_\sigma, t), \quad \varphi = \alpha_4(x_\nu)\psi(x_\tau, x_\sigma, t), \tag{3.9}$$

which is for an unplated region, and for a plated region the $\hat{\alpha}_j$, $\hat{\alpha}_4$ in (3.5) are appropriately modified and, accordingly, all quantities in (3.5) - (3.8) are written with bars on top and in place of (3.9) we have

$$\bar{u}_j = \bar{\alpha}_j(x_\nu)\bar{\psi}(x_\tau, x_\sigma, t), \quad \bar{\varphi} = \bar{\alpha}_4(x_\nu)\bar{\psi}(x_\tau, x_\sigma, t). \tag{3.10}$$

As in Ref.7 and in accordance with the explanation given there, we take the variations in the form

$$\delta u_j = \alpha_j^* \delta\psi^*, \quad \delta\varphi = \alpha_4^* \delta\psi^*,$$

$$\delta\bar{u}_j = \bar{\alpha}_j^* \delta\bar{\psi}^*, \quad \delta\bar{\varphi} = \bar{\alpha}_4^* \delta\bar{\psi}^*, \tag{3.11}$$

where the asterisk denotes complex conjugate and the variations in Eqs. (3.11) are consistent with the constraints. Moreover, it is to be noted that this choice of depth behavior for the variations results in surface wave equations in ψ and $\bar{\psi}$, each of which yields an expression for the time-average power flux identical with the one given by the three-dimensional equations, which is

$$P_j = \frac{1}{2}\,\mathrm{Re}\int (-T_{ji}\dot{u}_i^* + \varphi^*\dot{D}_j)\,dx_\nu. \tag{3.12}$$

Now, substituting from Eqs. (3.9) - (3.11) into Eq. (3.1), performing the integrations with respect to depth, and employing the planar divergence theorem, we obtain

$$\int_A [\rho H_{jj^*}\ddot{\psi} + T_\nu^S + D_\nu^S - T_{a,a}^S - D_{a,a}^S + \alpha_4^*(0)\hat{D}_\nu(0)]\delta\psi^* \, dA$$

$$+ \int_{\bar{A}} \{[\rho\bar{H}_{jj^*} + 2h'\rho'\bar{\alpha}_j(0)\alpha_j^*(0)]\ddot{\bar{\psi}} + \bar{T}_\nu^S + \bar{D}_\nu^S - \bar{T}_{a,a}^S - D_{a,a}^S$$

$$- 2h'[\lambda_o'\bar{\alpha}_a(0)\bar{\alpha}_b^*(0)\dot{\bar{\psi}}_{,ab} + \mu'(\bar{\alpha}_a(0)\bar{\psi}_{,ba} + \bar{\alpha}_b(0)\bar{\psi}_{,aa})\bar{\alpha}_b^*(0)]$$

$$+ \bar{\alpha}_4^*(0)\hat{\bar{D}}_\nu(0)\}\delta\bar{\psi}^* \, dA + \oint_C [n_a(T_a^S + D_a^S) - F^S + \Sigma^S]\,\delta\psi^* \, ds$$

$$+ \oint_{\bar{C}} \{\bar{n}_a(\bar{T}_a^S + \bar{D}_a^S + 2h'[\lambda_o'\bar{\alpha}_b(0)\bar{\alpha}_a^*(0)\bar{\psi}_{,b} + \mu'(\bar{\alpha}_a(0)\bar{\psi}_{,b}$$

$$+ \bar{\alpha}_b(0)\bar{\psi}_{,a})\bar{\alpha}_b^*(0)]) - \bar{F}^S + \bar{\Sigma}^S\}\delta\bar{\psi}^* \, ds - \int_{\ell_d} \{n_a^d(T_a^S + D_a^S - \bar{T}_a^S - \bar{D}_a^S$$

$$- 2h'[\lambda_o'\bar{\alpha}_b(0)\bar{\alpha}_a^*(0)\bar{\psi}_{,b} + \mu'(\bar{\alpha}_a(0)\bar{\psi}_{,b} + \bar{\alpha}_b(0)\bar{\psi}_{,a})\bar{\alpha}_b^*(0)])$$

$$- F^S + \Sigma^S + \bar{F}^S - \bar{\Sigma}^S\}\,\delta\psi^* \, ds, \qquad (3.13)$$

where n_a and $\bar{n}_a$ denote the components of the outwardly directed unit normals to the curves bounding the plated and unplated portions of the substrate, respectively, ℓ_d denotes the line separating the plated from the unplated region, n_a^d denotes the components of the unit normal to ℓ_d directed from the plated to the unplated region, it has been assumed that $\psi = \bar{\psi}$ along ℓ_d and

$$H_{jj^*} = \int_0^\infty \alpha_j\alpha_{j^*}dx_\nu, \quad T_\nu^S = \int_0^\infty \alpha_{j,\nu}^* T_{\nu j}\,dx_\nu,$$

$$D_\nu^S = \int_0^\infty \alpha_{4,\nu}^* D_\nu\,dx_\nu, \quad T_a^S = \int_0^\infty \alpha_j^* T_{aj}\,dx_\nu,$$

$$D_a^S = \int_0^\infty \alpha_4^* D_a\,dx_\nu, \quad F^S = \int_0^\infty \alpha_k^* t_k\,dx_\nu,$$

$$\Sigma^S = \int_0^\infty \sigma\alpha_4^*\,dx_\nu, \qquad (3.14)$$

for the unplated region and equivalent barred expressions exist for the plated region. Substituting from Eqs. (3.3), (3.8) and (3.9) into Eqs. (3.14) and integrating with respect to depth, we obtain

$$
\begin{aligned}
T^S_\nu &= c_{\nu jkb} H_{k;j^*,\nu} \psi_{,b} + c_{\nu;k\nu} H_{j^*,\nu;k,\nu} \psi + e_{b\nu j} H_{4;j^*,\nu} \psi_{,b} + e_{\nu\nu j} H_{j^*,\nu;4,\nu} \psi \,, \\
T^S_a &= c_{ajkb} H_{j^*k} \psi_{,b} + c_{ajk\nu} H_{j^*;k,\nu} \psi + e_{abj} H_{j^*4} \psi_{,b} + e_{\nu aj} H_{j^*;4,\nu} \psi \,, \\
D^S_\nu &= e_{\nu kb} H_{k;4^*,\nu} \psi_{,b} + e_{\nu k\nu} H_{4^*,\nu;k,\nu} \psi - \epsilon_{\nu b} H_{4^*;4,\nu} \psi_{,b} - \epsilon_{\nu\nu} H_{4^*,\nu;4,\nu} \psi \,, \\
D^S_a &= e_{akb} H_{4^*k} \psi_{,b} + e_{ak\nu} H_{4^*;k,\nu} \psi - \epsilon_{ab} H_{4^*4} \psi_{,b} - \epsilon_{a\nu} H_{4^*;4,\nu} \psi \,,
\end{aligned}
\tag{3.15}
$$

where

$$
\begin{aligned}
H_{\kappa\gamma^*} &= \int_0^\infty \alpha_\kappa \alpha^*_\gamma \, dx_\nu \,, \quad H_{\gamma^*\kappa} = \int_0^\infty \alpha^*_\gamma \alpha_\kappa \, dx_\nu \,, \\
H_{\kappa;\gamma^*,\nu} &= \int_0^\infty \alpha_\kappa \alpha^*_{\gamma,\nu} \, dx_\nu \,, \quad H_{\kappa^*;\gamma,\nu} = \int_0^\infty \alpha^*_\kappa \alpha_{\gamma,\nu} \, dx_\nu \,, \\
H_{\kappa^*,\nu;\gamma,\nu} &= \int_0^\infty \alpha^*_{\kappa,\nu} \alpha_{\gamma,\nu} \, dx_\nu \,, \quad H_{\gamma^*,\nu;\kappa,\nu} = \int_0^\infty \alpha^*_{\gamma,\nu} \alpha_{\kappa,\nu} \, dx_\nu \,,
\end{aligned}
\tag{3.16}
$$

$$
\kappa, \gamma = 1,2,3,4 \,. \tag{3.17}
$$

Equations (3.15), with Eqs. (3.16), are the surface wave constitutive equations for the approximate two-dimensional surface wave equations for an unplated region, and equivalent barred constitutive equations exist for a plated region. Since $\delta\psi^*$ and $\delta\bar{\psi}^*$ are arbitrary in the interior of the unplated and plated regions, respectively, we have the approximate one-dimensional surface wave differential equations

$$
T^S_{a,a} + D^S_{a,a} - T^S_\nu - D^S_\nu - \alpha^*_4(0)\hat{D}_\nu(0) = \rho H_{jj^*} \ddot{\psi} \,, \tag{3.18}
$$

$$
\begin{aligned}
\bar{T}^S_{a,a} + \bar{D}^S_{a,a} - \bar{T}^S_\nu - \bar{D}^S_\nu + 2h' [\lambda'_o \bar{\alpha}_a(0) \bar{\alpha}^*_b(0) \bar{\psi}_{,ab} + \mu' (\bar{\alpha}_a(0) \bar{\psi}_{,ba} + \delta_b(0) \bar{\psi}_{,aa}) \bar{\alpha}^*_b(0)] \\
= [\rho \bar{H}_{jj^*} + 2h' \rho' \bar{\alpha}_j(0) \bar{\alpha}^*_j(0)] \ddot{\bar{\psi}} \,,
\end{aligned}
\tag{3.19}
$$

in the respective regions, and where we have made use of the fact that $\bar{\alpha}_4^*(0) = 0$. Since $\delta\psi^*$ and $\delta\bar{\psi}^*$ are arbitrary on the cylindrical edges of the unplated and plated regions, respectively, we have the edge conditions

$$n_a(T_a^S + D_a^S) = F^S - \Sigma^S \ , \tag{3.20}$$

$$n_a[(\bar{T}_a^S + \bar{D}_a^S) + 2h'(\lambda_o'\bar{\alpha}_b(0)\bar{\alpha}_a^*(0)\bar{\psi}_{,b} + \mu'(\bar{\alpha}_a(0)\bar{\psi}_{,b} + \bar{\alpha}_b(0)\bar{\psi}_{,a})\bar{\alpha}_b^*(0))] = \bar{F}^S - \bar{\Sigma}^S \ . \tag{3.21}$$

Since $\delta\psi^*$ is arbitrary along ℓ_d, we have the continuity condition

$$n_a(T_a^S + D_a^S) = n_a[\bar{T}_a^S + \bar{D}_a^S + 2h'(\lambda_o'\bar{\alpha}_b(0)\bar{\alpha}_a^*(0)\bar{\psi}_{,b} + \mu'(\bar{\alpha}_a(0)\bar{\psi}_{,b} + \bar{\alpha}_b(0)\bar{\psi}_{,a})\bar{\alpha}_b^*(0))] \ , \tag{3.22}$$

at an edge separating a plated from an unplated region.

4. Transverse Modes in Reflective Arrays

In this section we apply the approximate two-dimensional surface wave equations derived in Sec.3 in the determination of the transverse modes propagating in the strips. We consider surface waves propagating in the digonal (x_1)-direction through a reflecting array on ST-cut quartz as shown in Fig.2 with 2w the width of each strip. A cross-section through a typical strip of the array is shown in Fig.5.

The differential equations are (3.18) for the unplated region with the α_j, α_4 known from Sec.2 for the free surface wave velocity V_o (horizontal line) in Fig.3 and (3.19) for the plated region with the $\bar{\alpha}_j$, $\bar{\alpha}_4$ known from Sec.2 for the velocity $\bar{V}$ labeled 2 in Fig.3, and with $\nu = 2$ in both regions. Since we are considering the special case of variable-crested surface waves propagating in the digonal direction on ST-cut quartz, a number of material constants in the surface wave constitutive equations in (3.15) vanish. Although we present the formal solution in the general case, the H.... defined in (3.16) simplify somewhat and may be written in the reduced form

$$H_{j^*k} = (K_{11^*}\delta_{j1} + \frac{\kappa^2}{\xi^2} K_{33^*}\delta_{j3})\delta_{k1} + \frac{\zeta^2}{\xi^2} K_{22^*}\delta_{k2}\delta_{j2}$$
$$+ (K_{33^*}\delta_{j3} + \frac{\kappa^2}{\xi^2} K_{11^*}\delta_{j1})\delta_{k3} ,$$

$$H_{k,2;j^*} = (K_{1,2;1^*}\delta_{j1} + \frac{\kappa^2}{\xi^2} K_{3,2;3^*}\delta_{j3})\delta_{k1} + \frac{\zeta^2}{\xi^2} K_{2,2;2^*}\delta_{k2}\delta_{j2}$$
$$+ (K_{3,2;3^*}\delta_{j3} + \frac{\kappa^2}{\xi^2} K_{1,2;1^*}\delta_{j1})\delta_{k3}$$
$$+ \frac{\zeta}{\xi} K_{1,2;2^*}\delta_{j2}\delta_{k1} + \frac{\zeta}{\xi} K_{2,2;1^*}\delta_{j1}\delta_{k2} ,$$

$$H_{k;j^*,2} = (K_{1;1^*,2}\delta_{j1} + \frac{\kappa^2}{\xi^2} K_{3;3^*,2}\delta_{j3})\delta_{k1} + \frac{\zeta^2}{\xi^2} K_{2;2^*,2}\delta_{k2}\delta_{j2}$$
$$+ (K_{3;3^*,2}\delta_{j3} + \frac{\kappa^2}{\xi^2} K_{1;1^*,2}\delta_{j1})\delta_{k3}$$
$$+ \frac{\zeta}{\xi} K_{2;1^*,2}\delta_{j1}\delta_{k2} + \frac{\zeta}{\xi} K_{1;1^*,2}\delta_{j2}\delta_{k1} ,$$

$$H_{k,2;j^*,2} = (K_{1,2;1^*,2}\delta_{j1} + \frac{\kappa^2}{\xi^2} K_{3,2;3^*,2}\delta_{j3})\delta_{k1}$$
$$+ \frac{\zeta^2}{\xi^2} K_{2,2;2^*:2}\delta_{k2}\delta_{j2} + (K_{3,2;3^*,2}\delta_{j3} + \frac{\kappa^2}{\xi^2} K_{1,2;1^*,2}\delta_{j1})\delta_{k3} ,$$

$$H_{4j^*} = K_{41^*}\delta_{1j} + \frac{\zeta}{\xi} K_{42^*}\delta_{j2} , \quad H_{44^*} = K_{44^*} ,$$

$$H_{4,2;j^*} = K_{4,2;1^*}\delta_{1j} + \frac{\zeta}{\xi} K_{4,2;2^*}\delta_{j2}$$

$$H_{k,2;4^*} = K_{1,2;4^*}\delta_{k1} + \frac{\zeta}{\xi} K_{2,2;4^*}\delta_{k2} , \quad H_{4,2;4^*,2} = K_{4,2;4^*,2} ,$$

$$H_{4,2;j^*,2} = K_{1,2;1^*,2}\delta_{j1} + \frac{\zeta}{\xi} K_{4,2;2^*,2}\delta_{j2} , \qquad (4.1)$$

where

$$K_{\kappa\gamma^*} = -\frac{1}{i\zeta}\sum_{n=1}^{4}\sum_{m=1}^{4}\frac{C^{(n)}C^{(m)*}A_\kappa^{(n)}A_\gamma^{(m)*}}{\beta_n-\beta_m^*},$$

$$K_{\kappa,2;\gamma^*} = -\sum_{n=1}^{4}\sum_{m=1}^{4}\frac{C^{(n)}C^{(m)*}A_\kappa^{(n)}A_\gamma^{(m)*}\beta_n}{\beta_n-\beta_m^*},$$

$$K_{\kappa;\gamma^*,2} = \sum_{n=1}^{4}\sum_{m=1}^{4}\frac{C^{(n)}C^{(m)*}A_\kappa^{(n)}A_\gamma^{(m)*}\beta_m^*}{\beta_n-\beta_m^*},$$

$$K_{\kappa,2;\gamma^*,2} = i\zeta\sum_{n=1}^{4}\sum_{m=1}^{4}\frac{C^{(n)}C^{(m)*}A_\kappa^{(n)}A_\gamma^{(m)*}\beta_n\beta_m^*}{\beta_n-\beta_m^*}. \qquad (4.2)$$

For the determination of the transverse modes propagating in the strips, the boundary conditions at the edge of the strips in the transverse direction are the continuity of Ψ, i.e.,

$$\Psi = \overline{\Psi}, \text{ at } x_3 = \pm w, \qquad (4.3)$$

and (3.22), which for the case at hand may be written in the form

$$\begin{aligned}
&c_{55}(H_{31^*}\Psi_{,1} + H_{11^*}\Psi_{,3}) + c_{56}(H_{1,2;1^*}\Psi + H_{21^*}\Psi_{,1}) + e_{25}H_{4,2;1^*}\Psi \\
&+ e_{35}H_{41^*}\Psi_{,3} + c_{14}H_{12^*}\Psi_{,1} + c_{24}H_{2,2;2^*}\Psi + c_{34}H_{32^*}\Psi_{,3} \\
&+ c_{44}(H_{22^*}\Psi_{,3} + H_{3,2;2^*}\Psi) + e_{14}H_{42^*}\Psi_{,1} + c_{13}H_{13^*}\Psi_{,1} \\
&+ c_{23}H_{2,2;3^*}\Psi + c_{33}H_{33^*}\Psi_{,3} + c_{34}(H_{23^*}\Psi_{,3} + H_{3,2;3^*}\Psi) + e_{31}H_{43^*}\Psi_{,1} \\
&+ e_{35}(H_{34^*}\Psi_{,1} + H_{14^*}\Psi_{,3}) + e_{36}(H_{1,2;4^*}\Psi + H_{24^*}\Psi_{,1}) \\
&- \epsilon_{23}H_{4,2;4^*}\Psi - \epsilon_{33}H_{44^*}\Psi_{,3}
\end{aligned}$$

$$= c_{55}(\bar{H}_{31^*}\bar{\Psi}_{,1} + \bar{H}_{11^*}\bar{\Psi}_{,3}) + c_{56}(\bar{H}_{1,2;1^*}\bar{\Psi} + \bar{H}_{21^*}\bar{\Psi}_{,1}) + e_{25}\bar{H}_{4,2;1^*}\bar{\Psi}$$
$$+ e_{35}\bar{H}_{41^*}\bar{\Psi}_{,3} + c_{14}\bar{H}_{12^*}\bar{\Psi}_{,1} + c_{24}\bar{H}_{2,2;2^*}\bar{\Psi} + c_{34}\bar{H}_{32^*}\bar{\Psi}_{,3}$$
$$+ c_{44}(\bar{H}_{22^*}\bar{\Psi}_{,3} + \bar{H}_{3,2;2^*}\bar{\Psi}) + e_{14}\bar{H}_{42^*}\bar{\Psi}_{,1} + c_{13}\bar{H}_{13^*}\bar{\Psi}_{,1} + c_{23}\bar{H}_{2,2;3^*}\bar{\Psi}$$
$$+ c_{33}\bar{H}_{33^*}\bar{\Psi}_{,3} + c_{34}(\bar{H}_{23^*}\bar{\Psi}_{,3} + \bar{H}_{3,2;3^*}\bar{\Psi}) + e_{31}\bar{H}_{43^*}\bar{\Psi}_{,1} + e_{35}(\bar{H}_{34^*}\bar{\Psi}_{,1}$$
$$+ \bar{H}_{14^*}\bar{\Psi}_{,3}) + e_{36}(\bar{H}_{1,2;4^*}\bar{\Psi} + \bar{H}_{24^*}\bar{\Psi}_{,1}) - \epsilon_{23}\bar{H}_{4,2;4^*}\bar{\Psi} - \epsilon_{33}\bar{H}_{44^*}\bar{\Psi}_{,3}$$
$$+ 2h'[\lambda'_o\vec{\alpha}_3(\bar{\alpha}_1\bar{\Psi}_{,1} + \bar{\alpha}_3\bar{\Psi}_{,3}) + \mu'(\bar{\alpha}_3\vec{\alpha}_1\bar{\Psi}_{,1} + 2\bar{\alpha}_3\vec{\alpha}_3\bar{\Psi}_{,3}$$
$$+ \bar{\alpha}_1\vec{\alpha}_1\bar{\Psi}_{,3})]_{x_2=0} \quad \text{at } x_3 = \pm w. \tag{4.4}$$

The surface wave solution functions may be written in the form

$$\Psi = Pe^{i\kappa x_3}e^{i(\xi x_1 - \omega t)}, \quad \bar{\Psi} = \bar{P}e^{i\bar{\kappa}x_3}e^{i(\xi x_1 - \omega t)}, \tag{4.5}$$

which satisfy (3.18) and (3.19), respectively, with (3.15) and the symmetry of ST-quartz, i.e., (4.1), provided

$$A\hat{\kappa}^4 + B\hat{\kappa}^3 + C\hat{\kappa}^2 + D\hat{\kappa} + E = 0, \tag{4.6}$$

$$\bar{A}\hat{\bar{\kappa}}^4 + \bar{B}\hat{\bar{\kappa}}^3 + \bar{C}\hat{\bar{\kappa}}^2 + \bar{D}\hat{\bar{\kappa}} + \bar{E} = 0, \tag{4.7}$$

where

$$\hat{\kappa} = \kappa/\zeta, \quad \hat{\bar{\kappa}} = \bar{\kappa}/\bar{\zeta}, \tag{4.8}$$

and

$$\bar{A} = (c_{33}\bar{h}_{11^*} + c_{55}\bar{h}_{33^*})\frac{\bar{\zeta}_o^2}{\xi^2} - i\bar{\gamma}((\lambda'_o + 2\mu')\bar{\alpha}_1\vec{\alpha}_1 + \mu'\bar{\alpha}_3\vec{\alpha}_3)_{x_2=0}\frac{\bar{\zeta}_o^2}{\xi^2},$$

$$\bar{B} = c_{34}i(\bar{h}_{21^*} - \bar{h}_{12^*})\frac{\bar{\zeta}_o^2}{\xi^2} + e_{35}i(\bar{h}_{43^*} - \bar{h}_{34^*})\frac{\bar{\zeta}_o}{\xi}$$
$$+ c_{34}(\bar{h}_{1;1^*,2} + \bar{h}_{1,2;1^*})\frac{\bar{\zeta}_o^2}{\xi^2} + c_{56}(\bar{h}_{3;3^*,2} + \bar{h}_{3,2;3^*})\frac{\bar{\zeta}_o^2}{\xi},$$

$$\bar{C} = c_{55}\bar{h}_{11^*} + e_{35}(\bar{h}_{41^*} + \bar{h}_{14^*}) + c_{44}\frac{\bar{\zeta}_o^2}{\xi^2}\bar{h}_{22^*} - \epsilon_{33}\bar{h}_{44^*} + c_{34}\frac{\bar{\zeta}_o}{\xi}(\bar{h}_{32^*} + \bar{h}_{23^*})$$
$$+ c_{33}h_{33^*} - i\bar{\gamma}((\lambda'_o + 2\mu')\bar{\alpha}_3\vec{\alpha}_3 + \mu'\bar{\alpha}_1\vec{\alpha}_1)_{x_2=0} + \frac{i\bar{\zeta}_o}{\xi}(c_{23}(\bar{h}_{2,2;1^*} - \bar{h}_{1;2^*,2})$$

$$+ c_{44}(\bar{h}_{2;1^*,2} - \bar{h}_{1,2;2^*}) + (e_{35} + e_{13})\,i(\bar{h}_{41^*} - \bar{h}_{14^*}) - \rho\bar{V}_o^2 \frac{\bar{\zeta}^2}{\xi^2}\bar{h}_{11^*}$$

$$+ i\bar{\gamma}\bar{V}_o^2\rho' \left.\frac{\bar{\zeta}^2}{\xi^2}\bar{\alpha}_1\bar{\alpha}_1^*\right|_{x_2=0} + c_{44}\frac{\bar{\zeta}^2}{\xi^2}\bar{h}_{1,2;1^*,2} + c_{55}\bar{h}_{11^*}$$

$$- i\bar{\gamma}\mu'\bar{\alpha}_1\bar{\alpha}_1^*\Big|_{x_2=0} - \rho\bar{V}_o^2\frac{\bar{\zeta}^2}{\xi^2}\bar{h}_{33^*} + i\bar{\gamma}\bar{V}_o^2\rho' \left.\frac{\bar{\zeta}^2}{\xi^2}\bar{\alpha}_3\bar{\alpha}_3^*\right|_{x_2=0}$$

$$+ c_{66}\frac{\bar{\zeta}^2}{\xi^2}\bar{h}_{3,2;3^*,2} + (c_{11}\bar{h}_{33^*} - i\bar{\gamma}(\lambda_o' + 2\mu')\bar{\alpha}_3\bar{\alpha}_3^*\Big|_{x_2=0}),$$

$$\bar{D} = c_{56}(\bar{h}_{1;1^*,2} + \bar{h}_{1,2;1^*}) + e_{36}(\bar{h}_{4;1^*,2} + \bar{h}_{1,2;4^*}) + e_{36}(\bar{h}_{4;1^*,2} + \bar{h}_{1,2;4^*})$$

$$+ c_{24}(\bar{h}_{2;2^*2} + \bar{h}_{2,2;2^*}) + e_{25}(\bar{h}_{1;4^*,2} + \bar{h}_{4,2;1^*}) - e_{23}(\bar{h}_{4;4^*,2} + \bar{h}_{4,2;4^*})$$

$$+ \frac{\xi}{\bar{\zeta}}((c_{14} + c_{56})(\bar{h}_{21^*} + \bar{h}_{12^*}) + (e_{14} + e_{36})(\bar{h}_{42^*} + \bar{h}_{24^*}) + c_{34}(\bar{h}_{3;3^*,2}$$

$$+ \bar{h}_{3,2;3^*}) + \frac{i\bar{\zeta}^2}{\xi^2}c_{24}(\bar{h}_{2,2;1^*,2} - \bar{h}_{1,2;2^*2}) + i(c_{56}(\bar{h}_{1,2;1^*} - \bar{h}_{1;1^*,2})$$

$$+ c_{14}(\bar{h}_{1;1^*,2} - \bar{h}_{1,2;1^*}) + e_{14}(\bar{h}_{4;1^*,2} - \bar{h}_{1,2;4^*}) + e_{25}(\bar{h}_{4,2;1^*} - \bar{h}_{1;4^*,2})$$

$$+ c_{56}(\bar{h}_{21^*} - \bar{h}_{12^*}) + c_{56}(\bar{h}_{3;3^*,2} - \bar{h}_{3,2;3^*}) + c_{14}(\bar{h}_{3,2;3^*} - \bar{h}_{3;3^*,2})),$$

$$\bar{E} = -\rho\bar{V}_o^2(\bar{h}_{11^*} + \frac{\bar{\zeta}^2}{\xi^2}\bar{h}_{22^*}) + i\bar{\gamma}\bar{V}_o^2\rho'(\bar{\alpha}_1\bar{\alpha}_1^* + \frac{\bar{\zeta}^2}{\xi^2}\bar{\alpha}_2\bar{\alpha}_2^*)_{x_2=0} + c_{66}\bar{h}_{1,2;1^*,2}$$

$$+ e_{26}(\bar{h}_{4,2;1^*,2} + \bar{h}_{1,2;4^*,2}) + c_{22}\bar{h}_{2,2;2^*,2}\frac{\bar{\zeta}^2}{\xi^2} - \epsilon_{22}\bar{h}_{4,2;4^*,2}$$

$$+ c_{66}(\bar{h}_{2;1^*,2} + \bar{h}_{1,2;2^*}) + c_{12}(\bar{h}_{1;2^*,2} + \bar{h}_{2,2;1^*}) + e_{12}(\bar{h}_{4;2^*,2} + \bar{h}_{2,2;4^*})$$

$$+ e_{26}(\bar{h}_{2;4^*,2} + \bar{h}_{4,2;2^*}) + \frac{\xi^2}{\bar{\zeta}^2}(c_{11}\bar{h}_{11^*} + e_{11}(\bar{h}_{41^*} + \bar{h}_{14^*}) + \frac{\bar{\zeta}^2}{\xi^2}c_{66}\bar{h}_{22^*}$$

$$- \epsilon_{11}\bar{h}_{44^*}) - i\bar{\gamma}\frac{\xi^2}{\bar{\zeta}^2}(\lambda_o' + 2\mu')\bar{\alpha}_1\bar{\alpha}_1^*\Big|_{x_2=0} - \rho\bar{V}_o^2\bar{h}_{33^*} + c_{44}\bar{h}_{3,2;3^*,2}$$

$$+ \frac{\xi^2}{\bar{\zeta}^2}c_{55}\bar{h}_{33^*} + i\bar{\gamma}(\rho'\bar{V}_o^2 - \frac{\xi^2}{\bar{\zeta}^2}\mu')\bar{\alpha}_3\bar{\alpha}_3^*\Big|_{x_2=0}, \qquad (4.9)$$

where the $\bar{h}$ .... in (4.9) are obtained from the expressions for the K.... in (4.2) by omitting the quantities outside the summation sign, $\bar{V}$ is known as a function of $\bar{\zeta}$ from the curve labeled 2 in Fig.3 and

$$\bar{\zeta}^2 = \xi^2 + \bar{\kappa}^2 , \quad \bar{\gamma} = 2\bar{\beta}h' . \tag{4.10}$$

The foregoing quantities in (4.9) and (4.10) are for the quartic for $\hat{\bar{\kappa}}$ in (4.7), which holds for the plated region. The expressions for A, B, C, D and E in the quartic for $\hat{\kappa}$ in (4.6), which holds for the unplated region, may be obtained from the expressions for $\bar{A}$, $\bar{B}$, $\bar{C}$, $\bar{D}$ and $\bar{E}$, respectively, simply by setting $h' = 0$, removing the bars in all remaining terms, adding the term

$$i\epsilon_o \alpha_4 \alpha_4^* \Big|_{x_2=0} , \tag{4.11}$$

to the expression for E and, of course, using the straight-crested solution for the unplated case from Sec.2, which corresponds to V_o given by the horizontal line in Fig.3.

Equations (4.6) and (4.7) are quasi-quartic equations in $\hat{\kappa}$ and $\hat{\bar{\kappa}}$, respectively. They are not absolute quartics because of the dependence of the coefficients on $\hat{\kappa}$ or $\hat{\bar{\kappa}}$. However, since in reflecting arrays the width of a strip is much larger than a propagation wavelength (or the spacing of the strips), we must have

$$|\hat{\kappa}| \ll 1 , \quad |\hat{\bar{\kappa}}| \ll 1 , \tag{4.12}$$

even for a relatively high order transverse mode. Hence, even though (4.6) and (4.7) are actually sixth-order equations in the problem, on account of (4.12) they may be treated as quartics here. Accordingly, for a given $\bar{\zeta}$, the complex quartic equation in (4.7) yields four complex roots for $\hat{\bar{\kappa}}$, two of which turn out to have a real part in the range of interest and an imaginary part at least an order of magnitude smaller than the real part.

In addition, the real parts are almost equal and opposite in sign. The other two roots have both real and imaginary parts outside the range of interest. We naturally ignore the latter two roots completely and neglect the small imaginary parts of each of the former. Similar statements hold in the case of Eq. (4.6) in $\hat{\varkappa}$, with the difference that in the two roots of interest the real parts are at least an order of magnitude smaller than the imaginary parts, which are almost equal and opposite in sign. In this case we neglect the small real parts of the roots of interest. Moreover, since the solution external to the strip must decay with distance from the edge, only the one decaying solution in each external region is employed. We deem the foregoing approximations to have essentially no influence on the accuracy of a calculation.

Since the frequency ω and the propagation wavenumber ξ are the same in the plated and unplated regions for any one transverse mode, from the assumed isotropic variable-cresting relations (3.6) and (4.10), we have

$$V_o\zeta = \xi V_t \ , \quad \bar{V}\bar{\zeta} = \xi V_t \ , \tag{4.13}$$

where V_t is the phase velocity of the particular transverse mode in question and V_o and $\bar{V}$ are found as functions of ζ and $\bar{\zeta}$ from the horizontal line and curve labeled 2, respectively, in Fig. 3. The associated $\varkappa$ and $\bar{\varkappa}$ are found from the izotropic variable-cresting relations in (3.6) and (4.10), respectively, for a given ξ, ζ and $\bar{\zeta}$.

We now take the solution of the boundary value problem in the form

$$\begin{aligned}
\psi_L &= P_1 e^{i\varkappa_1(x_3+w)} e^{i(\xi x_1-\omega t)} \ , \\
\bar{\psi} &= (\bar{P}_1 e^{i\bar{\varkappa}_1 x_3} + \bar{P}_2 e^{i\bar{\varkappa}_2 x_3}) e^{i(\xi x_1-\omega t)} \ , \\
\psi_R &= P_2 e^{i\varkappa_2(x_3-w)} e^{i(\xi x_1-\omega t)} \ ,
\end{aligned} \tag{4.14}$$

where κ_1, κ_2, $\bar{\kappa}_1$ and $\bar{\kappa}_2$ are the significant roots of (4.6) and (4.7) in accordance with the foregoing discussion. Substituting from (4.14) into (4.3) and (4.4), we obtain

$$\begin{bmatrix} C^{(11)} & C^{(12)} \\ C^{(21)} & C^{(22)} \end{bmatrix} \begin{bmatrix} \bar{P}_1 \\ \bar{P}_2 \end{bmatrix} = \begin{bmatrix} 0 \\ 0 \end{bmatrix} , \tag{4.15}$$

where

$$C^{(11)} = e^{-i\bar{\gamma}G\hat{\bar{\kappa}}_1}[(\bar{B}_1^{(1)} - B_1^{(1)}) + (\hat{\bar{\xi}}\bar{B}_2^{(1)} - \hat{\xi}B_2^{(1)}) + (\hat{\bar{\kappa}}_1\bar{B}_3^{(1)} - \hat{\kappa}_1 B_3^{(1)}) - i\bar{\gamma}(\hat{\bar{\xi}}\bar{B}_4^{(1)} + \hat{\bar{\kappa}}_1\bar{B}_5^{(1)})] ,$$

$$C^{(12)} = e^{-i\bar{\gamma}G\hat{\bar{\kappa}}_2}[(\bar{B}_1^{(2)} - B_1^{(1)}) + (\hat{\bar{\xi}}\bar{B}_2^{(2)} - \hat{\xi}B_2^{(1)}) + (\bar{\kappa}_2\bar{B}_3^{(2)} - \hat{\kappa}_1 B_3^{(1)}) - i\bar{\gamma}(\hat{\bar{\xi}}B_4^{(1)} + \hat{\bar{\kappa}}_2\bar{B}_5^{(2)})] ,$$

$$C^{(21)} = e^{i\bar{\gamma}G\hat{\bar{\kappa}}_1}[(\bar{B}_1^{(1)} - B_1^{(2)}) + (\hat{\bar{\xi}}\bar{B}_2^{(1)} - \hat{\xi}B_2^{(2)}) + (\hat{\bar{\kappa}}_1\bar{B}_3^{(1)} - \hat{\kappa}_2 B_3^{(2)}) - i\bar{\gamma}(\hat{\bar{\xi}}\bar{B}_4^{(1)} + \hat{\bar{\kappa}}_1\bar{B}_5^{(1)})] ,$$

$$C^{(22)} = e^{i\bar{\gamma}G\hat{\bar{\kappa}}_2}[(\bar{B}_1^{(2)} - B_1^{(2)}) + (\hat{\bar{\xi}}\bar{B}_2^{(2)} - \hat{\xi}B_2^{(2)}) + (\hat{\bar{\kappa}}_2\bar{B}_3^{(2)} - \hat{\kappa}_2 B_3^{(2)}) - i\bar{\gamma}(\hat{\bar{\xi}}\bar{B}_4^{(2)} + \hat{\bar{\kappa}}_2\bar{B}_5^{(2)})] ,$$

and

$$\hat{\xi} = \xi/\zeta , \quad \hat{\bar{\xi}} = \xi/\bar{\zeta} , \quad G = w/2h' , \tag{4.16}$$

and

$$\bar{B}_1 = c_{56}(\bar{h}_{1,2;1^*} + \frac{\bar{\kappa}^2}{\xi^2}\bar{h}_{3,2;3^*}) + e_{25}(\bar{h}_{4,2;1^*} + \frac{i\bar{\kappa}}{\xi}\bar{h}_{4,2;3^*}) + \frac{\bar{\zeta}^2}{\xi^2}\bar{h}_{2,2^*}$$
$$+ c_{44}\left(-\frac{i\bar{\kappa}\bar{\zeta}}{\xi^2}\bar{h}_{1,2;2^*} + \frac{\bar{\zeta}}{\xi}\bar{h}_{3,2;2^*}\right) + \frac{i\bar{\kappa}\bar{\zeta}}{\xi^2}c_{23}(\bar{h}_{2,2;1^*} + \bar{h}_{2,2;3^*})$$
$$+ \frac{\bar{\kappa}^2}{\xi^2}c_{34}(\bar{h}_{1,2;1^*} + \bar{h}_{3,2;3^*}) + e_{36}\bar{h}_{1,2;4^*} - e_{23}\bar{h}_{4,2;4^*} - e_{36}\frac{i\bar{\kappa}}{\xi}\bar{h}_{3,2;4^*}$$

$$\bar{B}_2 = c_{55}\frac{i\bar{\kappa}}{\xi}(\bar{h}_{33^*} - \bar{h}_{11^*}) + c_{56}\frac{\bar{\zeta}}{\xi}(\bar{h}_{21^*} + \frac{i\bar{\kappa}}{\xi}\bar{h}_{23^*}) + c_{14}\frac{\bar{\zeta}}{\xi}(\bar{h}_{12^*} - \frac{i\bar{\kappa}}{\xi}\bar{h}_{32^*})$$
$$+ c_{13}\frac{i\bar{\kappa}}{\xi}(\bar{h}_{11^*} - \bar{h}_{33^*}) + e_{35}(\bar{h}_{34^*} - \frac{i\bar{\kappa}}{\xi}\bar{h}_{14^*})$$
$$+ e_{13}(\bar{h}_{43^*} + \frac{i\bar{\kappa}}{\xi}\bar{h}_{41^*}) + e_{36}\frac{\bar{\zeta}}{\xi}\bar{h}_{24^*} + e_{14}\frac{\bar{\zeta}}{\xi}\bar{h}_{42^*}$$

$$\bar{B}_3 = c_{55}(\bar{h}_{11^*} + \frac{\bar{\kappa}^2}{\xi^2}\bar{h}_{33^*}) + e_{35}(\bar{h}_{41^*} + \frac{i\bar{\kappa}}{\xi}\bar{h}_{43^*})$$
$$+ c_{34}\frac{\bar{\zeta}}{\xi}(\bar{h}_{32^*} - \frac{i\bar{\kappa}}{\xi}\bar{h}_{12^*}) + \frac{\bar{\zeta}^2}{\xi^2}\bar{h}_{22^*} + c_{33}\left(\frac{\bar{\kappa}^2}{\xi^2}\bar{h}_{11^*} + \bar{h}_{33^*}\right)$$
$$+ c_{34}\frac{\bar{\zeta}}{\xi}(\bar{h}_{23^*} + \frac{i\bar{\kappa}}{\xi}\bar{h}_{21^*}) + e_{35}(\bar{h}_{14^*} - \frac{i\bar{\kappa}}{\xi}\bar{h}_{34^*}) - \epsilon_{33}\bar{h}_{4^*4}$$

$$\bar{B}_4 = \frac{i\bar{\kappa}}{\xi}(\lambda_o' - \mu')(\bar{\alpha}_1\bar{\alpha}_1^* - \bar{\alpha}_3\bar{\alpha}_3^*)_{x_2=0}$$

$$\bar{B}_5 = \left[(\lambda_o' + 2\mu')\bar{\alpha}_3\bar{\alpha}_3^* + \mu'\bar{\alpha}_1\bar{\alpha}_1^* + \frac{\bar{\kappa}^2}{\xi^2}\left((\lambda_o' + 2\mu')\bar{\alpha}_1\bar{\alpha}_1^* + \mu'\bar{\alpha}_3\bar{\alpha}_3^*\right)\right]_{x_2=0}, \qquad (4.17)$$

for the plated region, and the corresponding quantities B_1, B_2 and B_3 for the unplated region are obtained from $\bar{B}_1$, $\bar{B}_2$ and $\bar{B}_3$ in (4.17) simply by replacing the barred by unbarred quantities and, accordingly, using the appropriate quantities for the unplated region.

A calculation for the transverse modes propagating through the strips can now be performed by trial and error yielding $V_t = V_t(\xi)$ and satisfying (4.6), (4.7) and (4.15) along with (3.6) and $(4.10)_1$. Such calculations have been performed for shorted aluminum strips on ST-cut quartz, and the dispersion curves for the first nine symmetric modes are plotted in Fig.6 for G = 2100.

The boundary conditions at the edge of a strip in the propagation direction are the continuity of Ψ, i.e.,

$$\Psi = \bar{\Psi}, \quad \text{at } x_1 = \ell, \qquad (4.18)$$

and (3.22), which for propagation in the x_1-direction may be written in the form

$$
\begin{aligned}
&c_{11}H_{11}{}^{*}\Psi_{,1} + c_{12}H_{2,2;1}{}^{*}\Psi + c_{13}H_{31}{}^{*}\Psi_{,3} + c_{14}(H_{21}{}^{*}\Psi_{,3} + H_{3,2;1}{}^{*}\Psi) + e_{11}H_{41}{}^{*}\Psi_{,1} \\
&+ c_{56}(H_{32}{}^{*}\Psi_{,1} + H_{12}{}^{*}\Psi_{,3}) + c_{66}(H_{1,2;2}{}^{*}\Psi + H_{22}{}^{*}\Psi_{,1}) + e_{26}H_{4,2;2}{}^{*}\Psi \\
&+ e_{36}H_{42}{}^{*}\Psi_{,3} + c_{55}(H_{33}{}^{*}\Psi_{,1} + H_{13}{}^{*}\Psi_{,3}) + c_{56}(H_{1,2;3}{}^{*}\Psi + H_{23}{}^{*}\Psi_{,1}) \\
&+ e_{25}H_{4,2;3}{}^{*}\Psi + e_{35}H_{43}{}^{*}\Psi_{,3} + e_{11}H_{14}{}^{*}\Psi_{,1} + e_{12}H_{2,2;4}{}^{*}\Psi + e_{13}H_{34}{}^{*}\Psi_{,3} \\
&+ e_{14}(H_{24}{}^{*}\Psi_{,3} + H_{3,2;4}{}^{*}\Psi) - \epsilon_{11}H_{44}{}^{*}\Psi_{,1} \\
&= c_{11}\bar{H}_{11}{}^{*}\bar{\Psi}_{,1} + c_{12}\bar{H}_{2,2;1}{}^{*}\bar{\Psi} + c_{13}\bar{H}_{31}{}^{*}\bar{\Psi}_{,3} + c_{14}(\bar{H}_{21}{}^{*}\bar{\Psi}_{,3} + \bar{H}_{3,2;1}{}^{*}\bar{\Psi}) + e_{11}\bar{H}_{41}{}^{*}\bar{\Psi}_{,1} \\
&+ c_{56}(\bar{H}_{32}{}^{*}\bar{\Psi}_{,1} + \bar{H}_{12}{}^{*}\bar{\Psi}_{,3}) + c_{66}(\bar{H}_{1,2;2}{}^{*}\bar{\Psi} + \bar{H}_{22}{}^{*}\bar{\Psi}_{,1}) + e_{26}\bar{H}_{4,2;2}{}^{*}\bar{\Psi} \\
&+ e_{36}\bar{H}_{42}{}^{*}\bar{\Psi}_{,3} + c_{55}(\bar{H}_{33}{}^{*}\bar{\Psi}_{,1} + \bar{H}_{13}{}^{*}\bar{\Psi}_{,3}) + c_{56}(\bar{H}_{1,2;3}{}^{*}\bar{\Psi} + \bar{H}_{23}{}^{*}\bar{\Psi}_{,1}) \\
&+ e_{25}\bar{H}_{4,2;3}{}^{*}\bar{\Psi} + e_{35}\bar{H}_{43}{}^{*}\bar{\Psi}_{,3} + e_{11}\bar{H}_{14}{}^{*}\bar{\Psi}_{,1} + e_{12}\bar{H}_{2,2;4}{}^{*}\bar{\Psi} + e_{13}\bar{H}_{34}{}^{*}\bar{\Psi}_{,3} \\
&+ e_{14}(\bar{H}_{24}{}^{*}\bar{\Psi}_{,3} + \bar{H}_{3,2;4}{}^{*}\bar{\Psi}) - \epsilon_{11}\bar{H}_{44}{}^{*}\bar{\Psi}_{,1} + 2h'[\lambda_o'\vec{\alpha}_1(\bar{\alpha}_1\bar{\Psi}_{,1} + \bar{\alpha}_3\bar{\Psi}_{,3}) \\
&+ \mu'(2\vec{\alpha}_1\vec{\alpha}_1\bar{\Psi}_{,1} + \vec{\alpha}_1\vec{\alpha}_3\bar{\Psi}_{,3} + \vec{\alpha}_3\vec{\alpha}_3\bar{\Psi}_{,1})]_{x_2=0}, \quad \text{at } x_1 = \ell. \qquad (4.19)
\end{aligned}
$$

In order that the edge conditions (4.18) and (4.19) between a plated and unplated region of the array be satisfied pointwise, we take the transverse wavenumber in the interior of an unplated region to be the same as the transverse wavenumber $\bar{\varkappa}$ of that mode in the adjacent plated regions, where in accordance with the earlier discussion of the roots of (4.7), we have taken

$$\bar{\varkappa} = \frac{1}{2}\left[|\bar{\varkappa}_1| + |\bar{\varkappa}_2|\right]. \qquad (4.20)$$

Then since the usual isotropic variable-cresting relations (3.6) are taken to hold in the interior of an unplated region and the frequency is preserved, the resultant wavenumber ζ^U of the transverse mode in the interior of an unplated region is given by

$$\zeta^U = \overline{\zeta}\,\overline{V}/V\,, \tag{4.21}$$

where $\overline{V}$ and V are the straight-crested surface wave phase velocities at the respective resultant wavenumbers $\overline{\zeta}$ and ζ^U in the plated and unplated interior regions of the array and, as noted earlier, are plotted as the curves labeled 2 and 1, respectively, in Fig.3. The propagation wavenumber ξ_n^U of the nth transverse mode in the unplated region of the array is given by

$$\xi_n^U = \sqrt{(\zeta^U)^2 - \overline{\kappa}_n^2}\,, \tag{4.22}$$

which enables the phase velocity V_n^U of the nth transverse mode in the unplated region to be obtained from

$$V_n^U = \zeta^U V/\xi_n^U\,. \tag{4.23}$$

The transverse decay number in the exterior of an unplated region of the array is taken to be the same as the decay number κ of that mode in the exterior of the adjacent plated regions where in accordance with the earlier discussion of the roots of (4.6), we have taken

$$\kappa = \frac{1}{2}\left[\,|\kappa_1| + |\kappa_2|\,\right]\,. \tag{4.24}$$

This approximation, which results in any one transverse mode propagating through the reflecting array independent of all the other transverse modes, certainly has no real influence on the accuracy of a calculation within the framework of the procedure employed.

A plot of the fundamental transverse mode is shown as the dotted curve in Fig.7, which shows that the inflection points are at the edges of the strips. Since the transmitted power distribution depends on the square of the wave function $\overline{\Psi}(\phi)$, the transmitted power distribution of the fundamental transverse

mode takes the form shown as the solid curve in Fig.7, which indicates that the inflection points of the transverse power distribution are well inside the edges of the strips.

5. Reflection of a Rectangular Input

Since the width of the strips is very large compared to a wavelength or the spacing of the strips, the amplitude of each transverse mode very nearly vanishes at the edges of the strips. This fact is exhibited very clearly for the fundamental symmetric mode by the dotted curve in Fig.7. As a consequence of this, for simplicity, in the forced amplitude part of the analysis we take the transverse modes to have nodes at the edges of the strips. This approximation, which undoubtedly has a negligible influence on the accuracy of a calculation, enables the ordinary orthogonality relations for trigonometric functions to be used in the determination of the forcing amplitude of each transverse mode for an input of arbitrary shape in the transverse direction. Accordingly, when a symmetric input wave with an x_3-dependence of the form $f(x_3)$ is introduced, the amplitude a_n of the x_3-dependence of the nth symmetric mode may be written in the form

$$a_n \approx \frac{1}{w} \int_{-w}^{w} f(x_3)\cos \overline{\eta}_n x_3 \, dx_3 , \quad n = 1,3,5, \ldots , \tag{5.1}$$

and if

$$f(x_3) = 1 , \quad -w \le x_3 \le w , \quad f(x_3) = 0 , \quad |x_3| > w , \tag{5.2}$$

$$a_n \approx 4/n\pi . \tag{5.3}$$

Thus, for a rectangular input the weighting of each propagating essentially orthogonal symmetric transverse mode is given by (5.3), and the transmission and reflection of each separate transverse mode may be treated exactly as

in Ref.7. As in Ref.7 and for the same reasons, we must normalize (here) each of the transverse modes in the same way in the plated and unplated regions. Accordingly, we introduce the normalization conditions, which are equivalent to Eqs. (3.9) and (3.10) of Ref.7 and take the form

$$\alpha_1(0)\alpha_1(0) + \alpha_2(0)\alpha_2(0) + \alpha_3(0)\alpha_3(0) + \tilde{\alpha}_4(0)\tilde{\alpha}_4(0) = 1 , \tag{5.4}$$

in the unplated sections of the array and

$$\bar{\alpha}_1(0)\bar{\alpha}_1(0) + \bar{\alpha}_2(0)\bar{\alpha}_2(0) + \bar{\alpha}_3(0)\bar{\alpha}_3(0) + \tilde{\bar{\alpha}}_4(0)\tilde{\bar{\alpha}}_4(0) = 1 , \tag{5.5}$$

in the strips, where

$$\tilde{\alpha}_4(0) = (\epsilon_{22}/c_{66})^{\frac{1}{2}}\alpha_4(0) , \quad \tilde{\bar{\alpha}}_4(0) = (\epsilon_{22}/c_{66})^{\frac{1}{2}}\bar{\alpha}_4(0) . \tag{5.6}$$

Equations (5.4) and (5.5) are understood to represent n distinct normalization conditions, respectively, one for each of the n transverse modes. As in Ref.7, we now introduce the numbering system shown in Fig.8. Since there are n-strips, there are 2q + 1 distinct regions, the first of which is denoted o and the last of which, 2q. Note that the odd numbered regions are plated and the even, unplated. In order to obtain the transmission matrix for each transverse mode we consider the transmission and reflection across one typical strip denoted m with adjacent unplated regions (m - 1) and (m + 1). The surface wave solution functions of the approximate equations for the nth transverse mode for the three consecutive sections of the reflector may be written in the form

$$\begin{aligned}
\Phi^n_{m-1} &= \left[C^{n(1)}_{m-1} e^{i\xi_n(x_3 - z_m + d)} + C^{n(2)}_{m-1} e^{-i\xi_n(x_3 - z_m + d)}\right] e^{-i\omega t} , \\
\bar{\Phi}^n_m &= \left[\bar{C}^{n(1)}_m e^{i\xi_n(x_3 - z_m)} + \bar{C}^{n(2)}_m e^{-i\xi_n(x_3 - z_m)}\right] e^{-i\omega t} , \\
\Phi^n_{m+1} &= \left[C^{n(1)}_{m+1} e^{i\xi_n(x_3 - z_m - d)} + C^{n(2)}_{m+1} e^{-i\xi_n(x_3 - z_m - d)}\right] e^{-i\omega t} ,
\end{aligned} \tag{5.7}$$

$$z_m = (m-1)(\ell + d)/2 , \tag{5.8}$$

and $C_r^{n(1)}$ and $C_r^{n(2)}$ are the amplitudes of the positive and negative traveling nth transverse mode in the rth section. In accordance with Sec.4 each of the solution functions in (5.7) satisfies the appropriate equations in Sec.4 for the strips and the regions between the strips in the respective sections of the array provided the surface wave phase velocity dispersion curves $\bar{V}_n = \bar{V}(\bar{\xi}_n)$ and $V_n^U = V_n^U(\xi_n)$ are given by the appropriate curve in Fig.6 and Eqs. (4.21) - (4.23), respectively. The conditions to be satisfied at the junctions between the plated and unplated regions, i.e., at $x_1 = z_m$ and $x_1 = z_m + \ell$, are (4.18) and (4.19), which yield the four equations that enable us to express $C_{m+1}^{n(r)}$ in terms of $C_{m-1}^{n(s)}$ while eliminating the $\bar{C}_m^{n(t)}$, where r, s, t = 1, 2, and thus obtain the transmission matrix. Accordingly, substituting from (5.7) into (4.18) and (4.19), respectively, at $x_1 = z_m$ and $x_1 = z_m + \ell$, we obtain

$$\begin{aligned}
C_{m-1}^{n(1)} e^{i\xi_n d} + C_{m-1}^{n(2)} e^{-i\xi_n d} &= \bar{C}_m^{n(1)} + \bar{C}_m^{n(2)} , \\
M_n C_{m-1}^{n(1)} e^{i\xi_n d} + M_n^* C_{m-1}^{n(2)} e^{-i\xi_n d} &= \bar{M}_n \bar{C}_m^{n(1)} + \bar{M}_n^* \bar{C}_m^{n(2)} , \\
\bar{C}_m^{n(1)} e^{i\bar{\xi}_n \ell} + \bar{C}_m^{n(2)} e^{-i\bar{\xi}_n \ell} &= C_{m+1}^{n(1)} + C_{m+2}^{n(2)} , \\
\bar{M}_n \bar{C}_m^{n(1)} e^{i\bar{\xi}_n \ell} + \bar{M}_n^* \bar{C}_m^{n(2)} e^{-i\bar{\xi}_n \ell} &= M_n C_{m+1}^{n(1)} + M_n^* C_{m+1}^{n(2)} ,
\end{aligned} \tag{5.9}$$

where

$$\begin{aligned}
\bar{M}_n = -\Big(& \hat{c}_{12} \frac{\bar{\zeta}}{\bar{\xi}} \Big(\bar{h}_{2,2;1^*} + \frac{i\bar{\kappa}}{\bar{\xi}} \bar{h}_{2,2;3^*} \Big) + \hat{c}_{14} \frac{i\bar{\kappa}}{\bar{\xi}} (\bar{h}_{3,2;3^*} - \bar{h}_{1,2;1^*}) \\
& + \hat{c}_{66} \frac{\bar{\zeta}}{\bar{\xi}} \Big(\bar{h}_{1,2;2^*} - \frac{i\bar{\kappa}}{\bar{\xi}} \bar{h}_{3,2;2^*} \Big) + \hat{e}_{26} \frac{\bar{\zeta}}{\bar{\xi}} \bar{h}_{4,2;2^*} \\
& + \hat{c}_{56} \frac{i\bar{\kappa}}{\bar{\xi}} (\bar{h}_{1,2;1^*} - \bar{h}_{3,2;3^*}) + \hat{e}_{25} \Big(\bar{h}_{4,2;3^*} + \frac{i\bar{\kappa}}{\bar{\xi}} \bar{h}_{4,2;1^*} \Big)
\end{aligned}$$

$$+ \hat{e}_{12} \frac{\bar{\zeta}}{\xi} \bar{h}_{2,2;4^*} + \hat{e}_{14} \left(\bar{h}_{3,2;4^*} - \frac{i\bar{\kappa}}{\xi} \bar{h}_{1,2;4^*} \right) \Big)$$

$$- \frac{\bar{\kappa}}{\bar{\zeta}} \Big(\hat{c}_{13} \frac{i\bar{\kappa}}{\xi} (\bar{h}_{33^*} - \bar{h}_{11^*}) + \hat{c}_{14} \frac{\bar{\zeta}}{\xi} \left(\bar{h}_{21^*} + \frac{i\bar{\kappa}}{\xi} \bar{h}_{23^*} \right)$$

$$+ \hat{c}_{56} \frac{\bar{\zeta}}{\xi} \left(\bar{h}_{12^*} - \frac{i\bar{\kappa}}{\xi} \bar{h}_{32^*} \right) + \hat{e}_{26} \frac{\bar{\zeta}}{\xi} \bar{h}_{42^*}$$

$$+ \hat{c}_{55} \frac{i\bar{\kappa}}{\xi} (\bar{h}_{11^*} - \bar{h}_{33^*}) + \hat{e}_{35} \left(\bar{h}_{43^*} - \frac{i\bar{\kappa}}{\xi} \bar{h}_{41^*} \right)$$

$$+ \hat{e}_{13} \left(\bar{h}_{34^*} - \frac{i\bar{\kappa}}{\xi} \bar{h}_{14^*} \right) + e_{14} \frac{\bar{\zeta}}{\xi} \bar{h}_{24^*} \Big)$$

$$- \frac{\xi}{\bar{\zeta}} \Big(\hat{c}_{11} \left(\bar{h}_{11^*} + \frac{\bar{\kappa}^2}{\xi^2} \bar{h}_{33^*} \right) + \hat{c}_{66} \frac{\bar{\zeta}^2}{\xi^2} \bar{h}_{22^*} + \hat{c}_{55} \left(\bar{h}_{33^*} + \frac{\bar{\kappa}^2}{\xi^2} \bar{h}_{11^*} \right) - \hat{\epsilon}_{11} \bar{h}_{44^*}$$

$$+ \hat{e}_{11} \left(\bar{h}_{41^*} + \frac{i\bar{\kappa}}{\xi} \bar{h}_{43^*} + \bar{h}_{14^*} - \frac{i\bar{\kappa}}{\xi} \bar{h}_{34^*} \right)$$

$$+ \hat{e}_{56} \frac{\bar{\zeta}}{\xi} \left(\bar{h}_{23^*} + \frac{i\bar{\kappa}}{\xi} \bar{h}_{21^*} + \bar{h}_{32^*} - \frac{i\bar{\kappa}}{\xi} \bar{h}_{12^*} \right) \Big)$$

$$+ i2h' \xi \hat{\mu}' \Big(\Big(1 + \Big(\frac{3\lambda' + 2\mu'}{\lambda' + 2\mu'} \Big) \Big) (\bar{\alpha}_1^*(0) \bar{\alpha}_1(0) + \frac{\bar{\kappa}^2}{\xi^2} \bar{\alpha}_3^*(0) \bar{\alpha}_3(0) \Big)$$

$$+ \bar{\alpha}_3^*(0) \bar{\alpha}_3(0) + \frac{\bar{\kappa}^2}{\xi^2} \bar{\alpha}_1^*(0) \bar{\alpha}_1(0) \Big)$$

$$+ i2h' \bar{\kappa} (\lambda_o' - \mu') (\bar{\alpha}_3^*(0) \bar{\alpha}_3(0) - \bar{\alpha}_1^*(0) \bar{\alpha}_1(0)) \frac{i\bar{\kappa}}{\xi} \quad , \tag{5.10}$$

where all the appropriate quantities on the right-hand side are understood to be for the nth transverse mode and for convenience we have suppressed the n and $\bar{M}_n$ reduces to M_n when $h' = 0$ and the dimensionless material constants

$$\hat{c}_{pq} = c_{pq}/c_{66} \, , \quad \hat{e}_{ip} = e_{ip}/\sqrt{c_{66}\epsilon_{22}} \, , \quad \hat{\epsilon}_{ij} = \epsilon_{ij}/\epsilon_{22} \, , \quad \hat{\mu}' = \mu'/c_{66} \, , \tag{5.11}$$

have been introduced. Solving the four linear algebraic equations in (5.9) for $C_{m+1}^{n(r)}$ in terms of $C_{m-1}^{n(s)}$, we obtain

$$C_{m+1}^{n(r)} = \sum_{s=1}^{2} T_n^{(rs)} C_{m-1}^{n(s)} \, , \tag{5.12}$$

where

$$T_n^{(11)} = \Big[(M_n^* - \bar{M}_n)(\bar{M}_n^* - M_n) e^{i(\bar{\xi}_n \ell + \xi_n d)} + (M_n^* - \bar{M}_n^*)(M_n - \bar{M}_n) e^{i(\xi_n d - \bar{\xi}_n \ell)} \Big] / (M_n^* - M_n)(\bar{M}_n^* - \bar{M}_n) ,$$

$$T_n^{(12)} = \Big[(M_n^* - \bar{M}_n)(\bar{M}_n^* - M_n^*) e^{i(\bar{\xi}_n \ell - \xi_n d)} + (M_n^* - \bar{M}_n^*)(M_n^* - \bar{M}_n) e^{-i(\bar{\xi}_n \ell + \xi_n d)} \Big] / (M_n^* - M_n)(\bar{M}_n^* - \bar{M}_n) ,$$

$$T_n^{(21)} = \Big[(M_n - \bar{M}_n)(M_n - \bar{M}_n^*) e^{i(\bar{\xi}_n \ell + \xi_n d)} + (M_n - \bar{M}_n^*)(\bar{M}_n - M_n) e^{i(\xi_n d - \bar{\xi}_n \ell)} \Big] / (M_n^* - M_n)(\bar{M}_n^* - \bar{M}_n) ,$$

$$T_n^{(22)} = \Big[(\bar{M}_n - M_n)(\bar{M}_n^* - M_n^*) e^{i(\bar{\xi}_n \ell - \xi_n d)} + (\bar{M}_n^* - M_n)(M_n^* - \bar{M}_n) e^{-i(\bar{\xi}_n \ell + \xi_n d)} \Big] / (M_n^* - M_n)(\bar{M}_n^* - \bar{M}_n) , \quad (5.13)$$

which shows that $T_n^{(rs)}$ is hermitian. At this point it is both conventional and convenient to suppress the indices on the 2×2 matrix $T_n^{(rs)}$ and 1×2 column vectors $C_{m+1}^{n(r)}$ and $C_{m-1}^{n(s)}$ and write

$$C_{m+1}^{n} = T_n C_{m-1}^{n} . \quad (5.14)$$

Since this analysis holds for each strip, application of (5.14) successively across all the strips in the array from the first to the last yields

$$C_{2q} = \overbrace{T_n T_n T_n T_n \ldots . T_n}^{q \text{ times}} C_o . \quad (5.15)$$

Since $C_{2q}^{(2)}$ vanishes and $C_o^{n(1)} = C^o a_n$ is known, where C^o is the amplitude of the rectangular input, (5.15) constitutes two linear inhomogeneous algebraic equations in $C_{2q}^{n(1)}$ and $C_o^{n(2)}$, which may readily be solved. More specifically, if we define $S_n^{(rs)}$ by

$$S_n^{(rs)} = [T_n^q]^{rs} , \quad (5.16)$$

the matrix equation (5.15) yields

$$C_o^{n(2)} = -(S_n^{(21)}/S_n^{(22)})C_o^{n(1)}, \quad C_{2q}^{n(1)} = [S_n^{(11)} - S_n^{(12)}S_n^{(21)}/S_n^{(22)}]C^o a_n, \qquad (5.17)$$

which gives the amplitudes $C_o^{n(2)}$ and $C_{2q}^{n(1)}$ of the nth transverse mode reflected and transmitted, respectively, in terms of the amplitude of the incident transversely uniform surface wave. Calculations may now readily be performed. When a calculation has been performed, the power reflection coefficient R_p for the nth transverse mode defined by

$$R_p^n = 10 \log_{10}(C_o^{n(2)}C_o^{n(2)*}/C_o^{n(1)}C_o^{n(1)*}), \qquad (5.18)$$

and the power transmission coefficient T_p for the nth transverse mode

$$T_p^n = 10 \log_{10}C_{2q}^{n(1)}C_{2q}^{n(1)*}/C_o^{n(1)}C_o^{n(1)*}), \qquad (5.19)$$

both in dB, may readily be evaluated. Clearly, the calculated response is the simple sum of all the reflection amplitudes resulting from the rectangular input which is essentially what is measured in a typical surface wave resonator experiment. The first nine symmetric modes have been included in all calculations performed here. Calculations have been performed for a surface wave reflector consisting of 200 aluminum strips, 10,000 Å thick deposited on ST-cut quartz subject to a rectangular input. The center frequency of the fundamental mode is 74.7 MHz. The resulting power reflection coefficient is plotted in Fig.9. The curve clearly reveals the existence of small resonance peaks (or spurs) on the high frequency side of the fundamental resonance which were observed by Staples and Smythe[17]. The calculated resonances normalized with respect to the fundamental resonance are compared with the measured results of Staples and Smythe[17] in Table I. The calculated values are somewhat below the measured values. We believe the agreement would be improved considerably if a more accurate dispersion curve for the aluminum film on the

quartz substrate were employed because the film thickness-to-wavelength ratios used in the experiments were a little too large at the resonances for the thin film approximation employed in the calculations. In Fig.10 we have plotted the amplitude and power reflection coefficients for the fundamental mode as a function of the number of strips along with the same quantities obtained from our earlier[7] straight-crested analysis. It is clear from the figure that the earlier treatment overestimated the results. This is a result of the newly defined straight-crested phase velocities in the plated and unplated regions of the array. Figures 11-13, respectively, contain power transmission, power reflection coefficients and the phase of the reflected wave, all for the fundamental transverse mode.

Acknowledgements

We wish to thank M. Sack for help with the calculations.

This work was supported in part by the Office of Naval Research under Contract No. N00014-76-C-0368.

REFERENCES

1. E.K. Sittig and G.A. Coquin, "Filters and Dispersive Delay Lines Using Repetitively Mismatched Ultrasonic Transmission Lines," IEEE Trans. Sonics Ultrason., SU-15, 111 (1968).

2. E.J. Staples, J.S. Schoenwald, R.C. Rosenfeld and C.S. Hartmann, "UHF Surface Acoustic Wave Resonators," 1974 Ultrasonics Symposium Proceedings, IEEE Cat. No. 74 CHO 894-1SU, Institute of Electrical and Electronics Engineers, New York, 245 (1974).

3. R.C. Williamson and H.I. Smith, "The Reflection of Elastic Surface Waves from Periodic Arrays on YZ $LiNbO_3$," presented at the IEEE Ultrasonics Symposium, Miami, 1971, Paper J-5.

4. J. Melngailis, J.M. Smith and J.H. Cafarella, "Bandpass Surface Wave Filters," 1972 Ultrasonics Symposium Proceedings, IEEE Cat. No. 72 CHO 708-8SU, Institute of Electrical and Electronics Engineers, New York, 221 (1972).

5. R.C.M. Li, "Analysis of Surface Wave Reflection from a Periodic Array of Grooves," 1972 Ultrasonics Symposium Proceedings, IEEE Cat. No. 72 CHO 807-8SU, Institute of Electrical and Electronics Engineers, New York, 263 (1972).

6. R.C.M. Li and J. Melngailis, "Second-Order Effects in Surface-Wave Devices due to Stored Energy at Step Discontinuities," 1973 Ultrasonics Symposium Proceedings, IEEE Cat. No. 73 CHO 807-8SU, Institute of Electrical and Electronics Engineers, New York, 503 (1973).

7. B.K. Sinha and H.F. Tiersten, "A Variational Analysis of the Reflection of Surface Waves by Arrays of Reflecting Strips," J. Appl. Phys., 47, 2824 (1976).

8. T. Yoneyama and S. Nishida, "Reflection and Transmission of Rayleigh Waves by the Edge of a Deposited Thin Film," J. Acoust. Soc. Am., 55, 738 (1974).

9. H.S. Tuan and R.C.M. Li, "Rayleigh-Wave Reflection from Groove and Step Discontinuities," J. Acoust. Soc. Am., 55, 1212 (1974).

10. D.A. Simons, "Reflection of Rayleigh Waves by Strips, Grooves and Periodic Arrays of Strips or Grooves," J. Acoust. Soc. Am., 63, 1292 (1978).

11. H.F. Tiersten and R.C. Smythe, "Guided Acoustic Surface Wave Filters," Appl. Phys. Lett., 28, 111 (1976).

12. H.A. Haus, "Modes in SAW Grating Resonators," Electronics Letters, 13, 12 (1977).

13. H.A. Haus, "Modes in SAW Grating Resonators," J. Appl. Phys., 49, (1978).

14. O. Schwelb, E.L. Adler and G.W. Farnell, "Effect of Anisotropy on Waveguide Modes in SAW Resonators," 1977 Ultrasonics Symposium Proceedings, IEEE Cat. No. 77 CHO 1264-1SU, Institute of Electrical and Electronics Engineers, New York, 867 (1977).

15. H.F. Tiersten, "Elastic Surface Waves Guided by Thin Films," J. Appl. Phys., 40, 770 (1969).

16. B.K. Sinha and H.F. Tiersten, "Elastic and Piezoelectric Surface Waves Guided by Thin Films," J. Appl. Phys., 44, 4831 (1973).

17. E.J. Staples and R.C. Smythe, "Surface Acoustic Wave Resonators on ST-Quartz," 1975 Ultrasonics Symposium Proceedings, IEEE Cat. No. 75 CHO 994-4SU, Institute of Electrical and Electronics Engineers, New York, 307 (1975).

18. R.D. Mindlin, "High Frequency Vibrations of Plated, Crystal Plates," Progress in Applied Mechanics (MacMillan, New York, 1963), pp.73-84.

19. L.A. Coldren, H.A. Haus and K.L. Wang, "Experimental Verification of Mode Shape in SAW Grating Resonators," Electronics Letters, 13, 642 (1977).

20. H.F. Tiersten and B.K. Sinha, "A Perturbation Analysis of the Attenuation and Dispersion of Surface Waves," J. Appl. Phys., 49, 87 (1978).

21. The mean phase velocity is meaningful when the wavelength is of the order of the spacing between the strips or larger, but not when it is much smaller.

TABLE I

Mode	F/F_o	Staples and Smythe
1	1	1
2	1.00013	1.00018
3	1.00032	1.0004
4	1.00065	1.0008
5	1.000935	1.0012
6	1.0015	1.0019
7	1.002	1.0028

FIGURE CAPTIONS

Figure 1 Lowest Straight-Crested Phase Velocity Dispersion Curve for an Aluminum Film on ST-Cut Quartz

Figure 2 Schematic Diagram of a Surface-Wave Reflector

Figure 3 Straight-Crested Phase Velocity Dispersion Curves in Both the Plated with Adjacent Unplated and Unplated with Adjacent Plated Regions for the case $d = \ell$. The dispersion curve from Fig.1 is plotted in this figure.

Figure 4 Diagram Showing a Partially Plated and Partially Unplated Substrate Bounded by a Cylindrical Surface

Figure 5 Cross-Section through a Typical Strip in the Array

Figure 6 Phase Velocity Dispersion Curves for G = 2100 for the First Nine Symmetric Modes

Figure 7 Transverse Distribution of the Surface Wave Function and the Power Flux for the Fundamental Mode

Figure 8 Diagram Showing the Numbering Scheme for the Transmission Matrices

Figure 9 Power Reflection Coefficient of a Surface-Wave Reflector with 200 Aluminum Strips 10,000 Å Thick on ST-Cut Quartz at a Fundamental Frequency of 74.7 MHz for a Rectangular Input. Results are for $d = \ell$ and $2w = 100\ \lambda_R$.

Figure 10 Amplitude (A_1) and Power (B_1) Reflection Coefficients of the Fundamental Mode of the Surface-Wave Reflector with 10,000 Å Thick Aluminum Strips at a Center Frequency of 74.7 MHz, as a Function of the Number of Strips. The curves A and B are obtained using the straight-crested procedure presented in Ref.7.

Figure 11 Power Transmission Coefficient of the Fundamental Mode of the Surface-Wave Reflector

Figure 12 Power Reflection Coefficient of the Fundamental Mode of the Surface-Wave Reflector

Figure 13 Phase of the Fundamental Reflected Wave

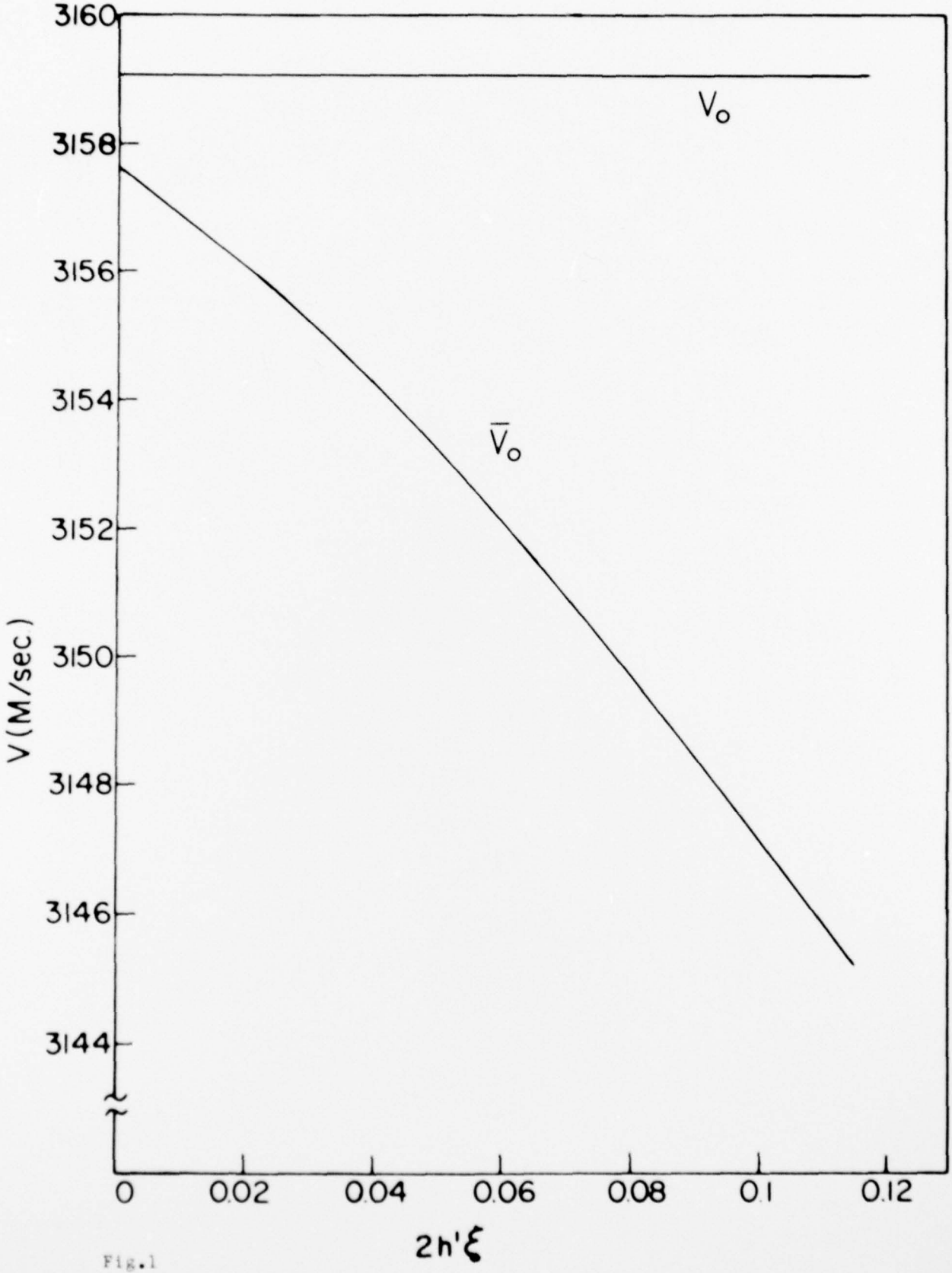
3160
3158
3156
3154
3152
3150
3148
3146
3144
V (M/sec)
V_o
$\bar{V}_o$
0
0.02
0.04
0.06
0.08
0.1
0.12
$2h'\xi$

Fig.1

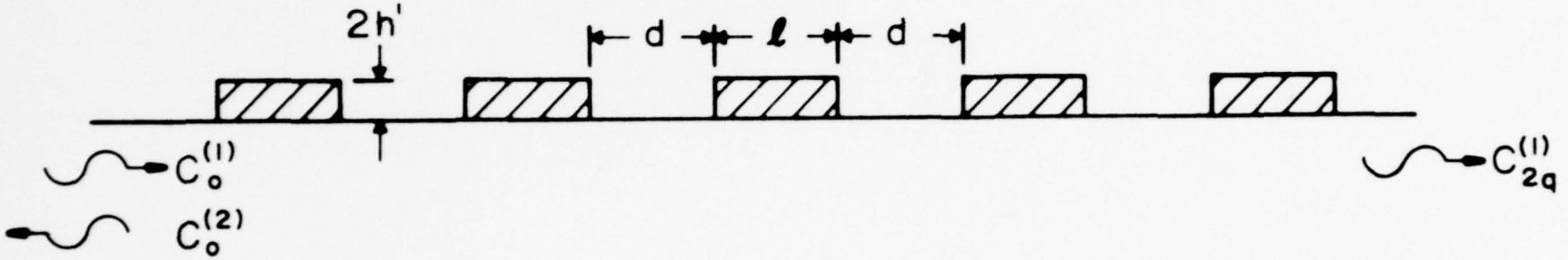

Fig.2

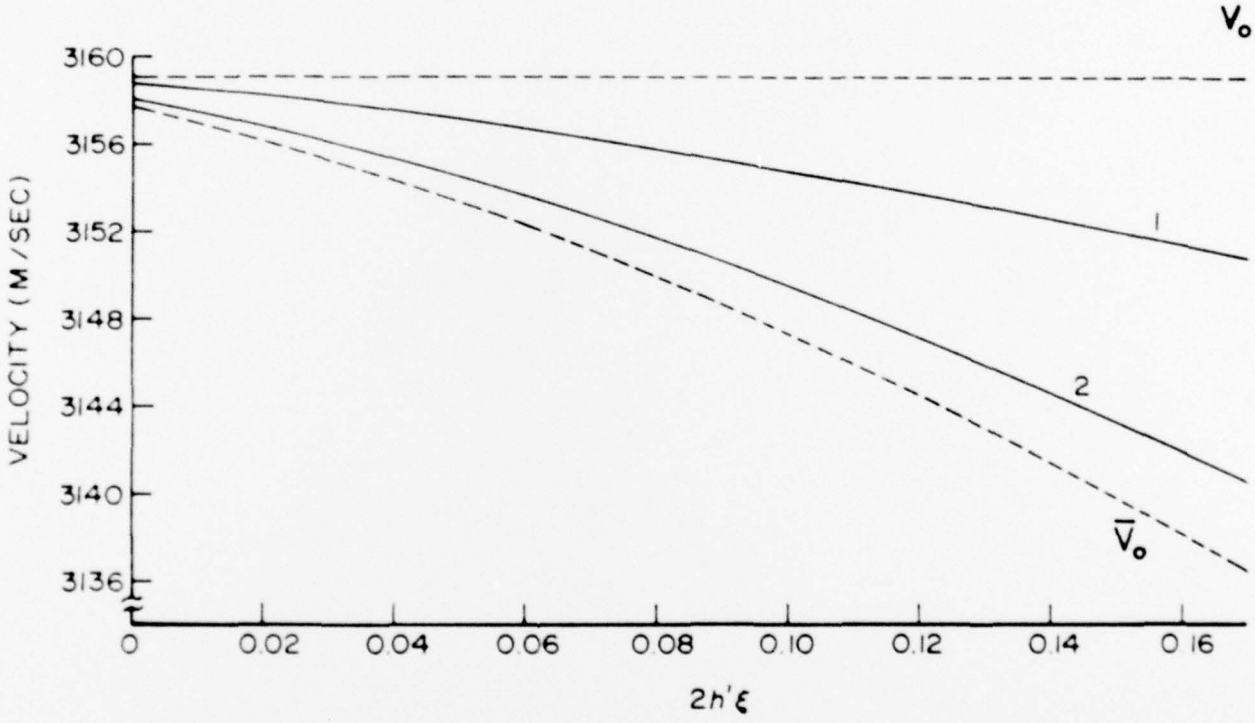
V_o
3160
3156
3152
3148
3144
3140
3136
VELOCITY (M/SEC)
1
2
$\bar{V}_o$
0
0.02
0.04
0.06
0.08
0.10
0.12
0.14
0.16
$2h'\xi$

Fig.3

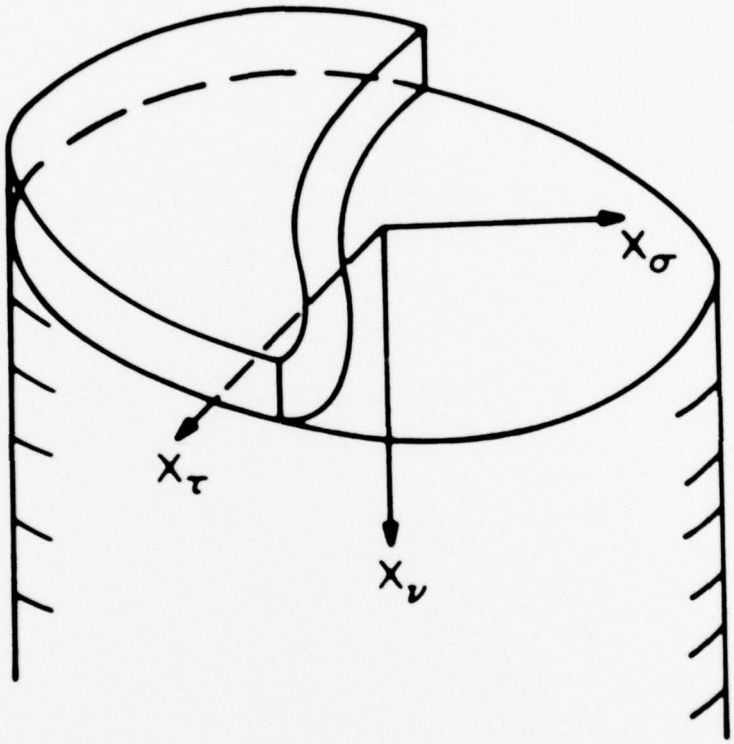

Fig.4

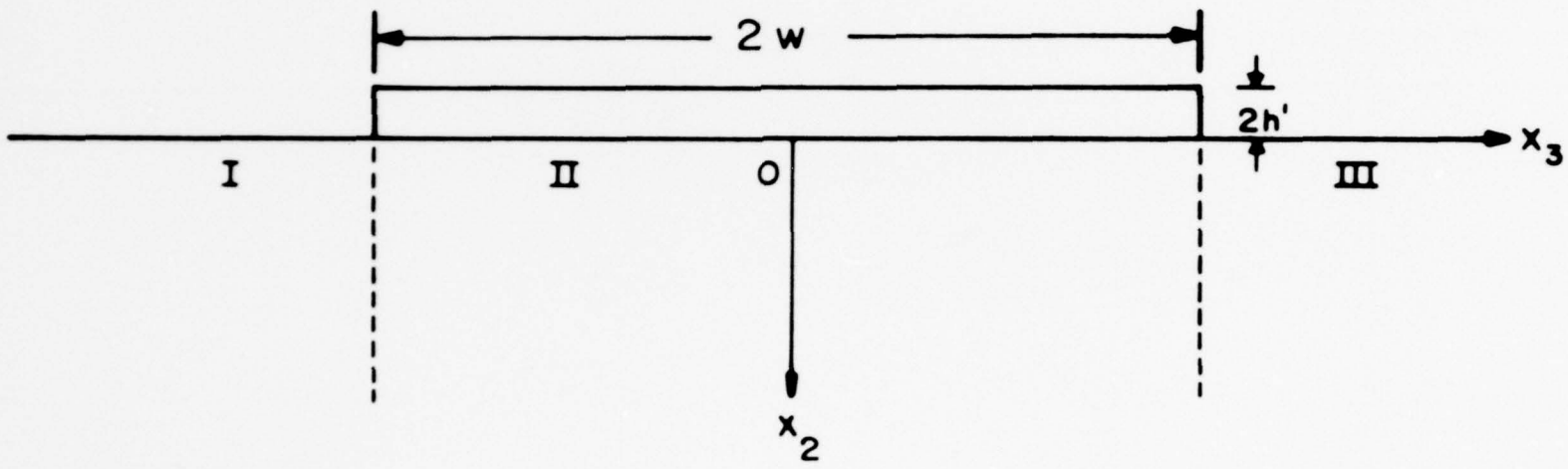

Fig.5

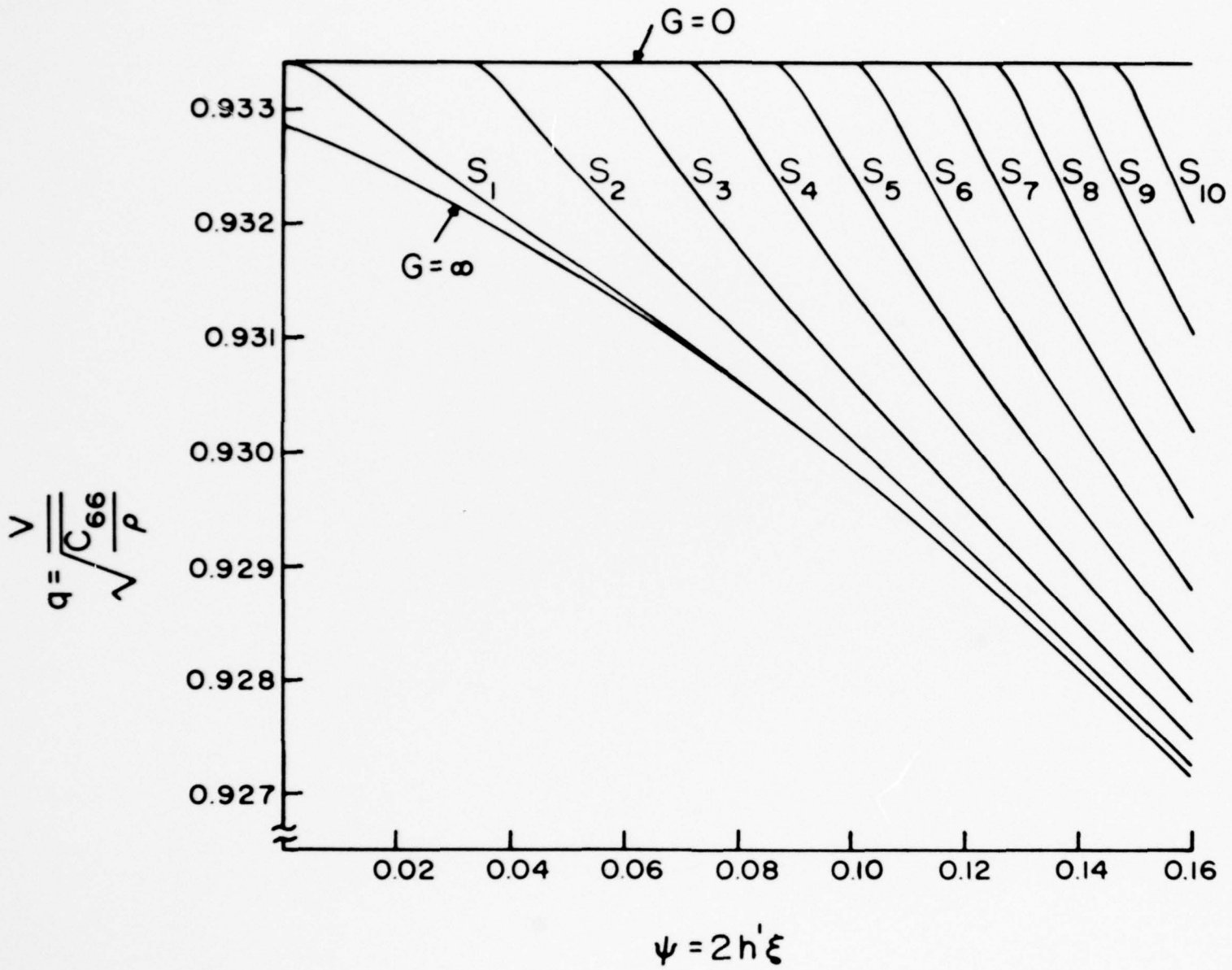
G=0
G=∞
S1
S2
S3
S4
S5
S6
S7
S8
S9
S10
0.933
0.932
0.931
0.930
0.929
0.928
0.927
0.02
0.04
0.06
0.08
0.10
0.12
0.14
0.16
$q = \frac{V}{\sqrt{\left|\frac{C_{66}}{\rho}\right|}}$
$\psi = 2h'\xi$

Fig.6

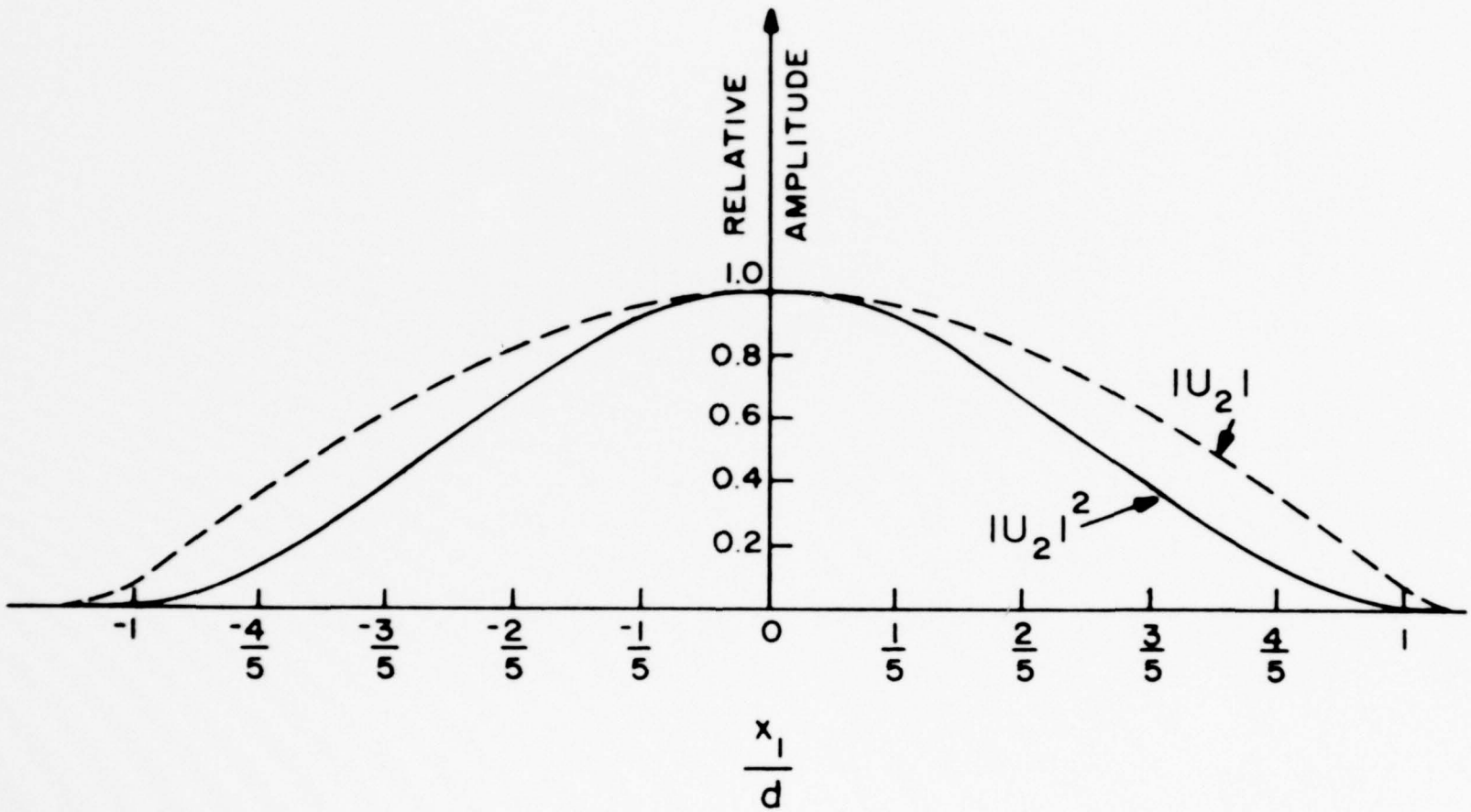
RELATIVE AMPLITUDE
1.0
0.8
0.6
0.4
0.2
$|U_2|$
$|U_2|^2$
-1
$-\frac{4}{5}$
$-\frac{3}{5}$
$-\frac{2}{5}$
$-\frac{1}{5}$
0
$\frac{1}{5}$
$\frac{2}{5}$
$\frac{3}{5}$
$\frac{4}{5}$
1
$\frac{x_1}{d}$

Fig.7

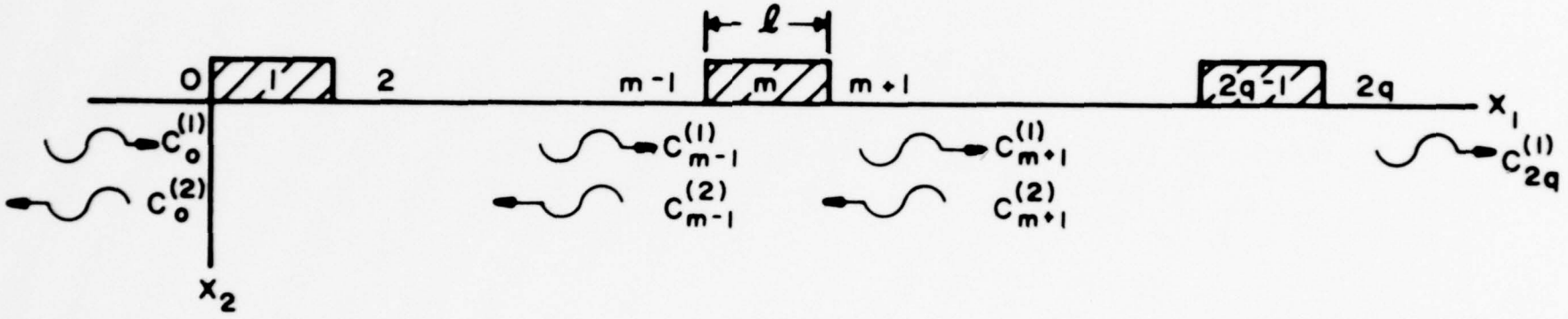

Fig. 8

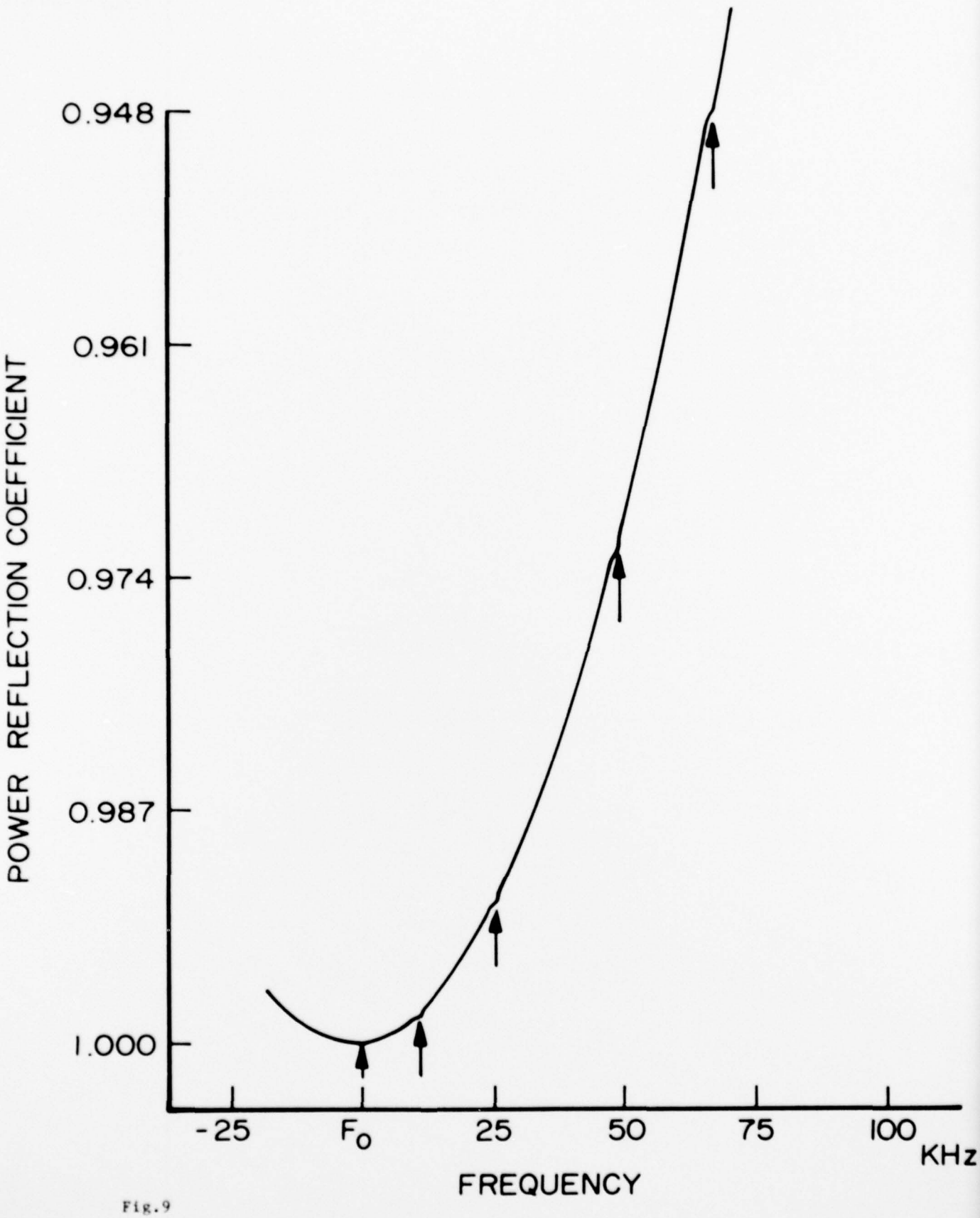
0.948
0.961
0.974
0.987
1.000
POWER REFLECTION COEFFICIENT
-25
F_o
25
50
75
100
KHz
FREQUENCY

Fig.9

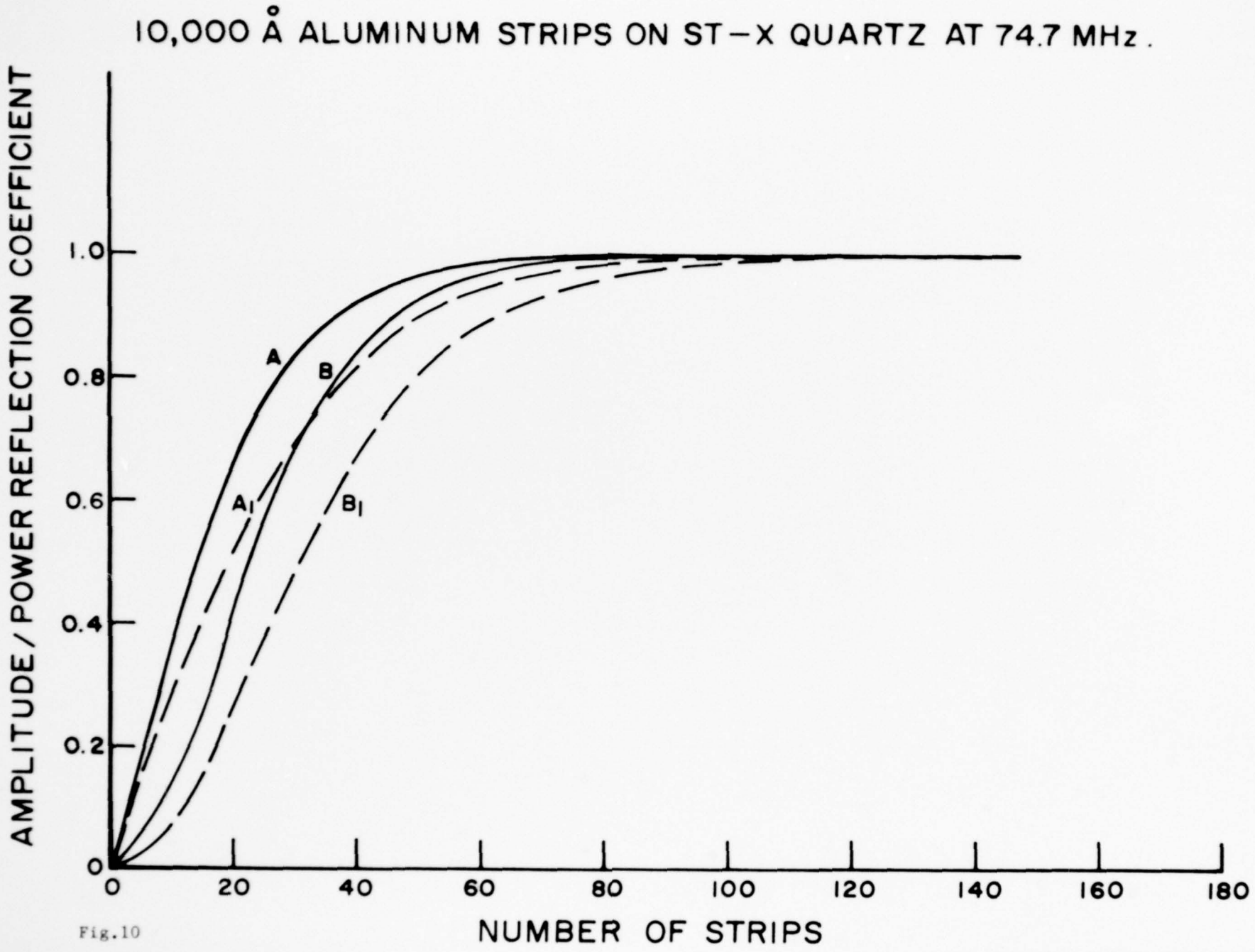
10,000 Å ALUMINUM STRIPS ON ST−X QUARTZ AT 74.7 MHz.
AMPLITUDE / POWER REFLECTION COEFFICIENT
1.0
0.8
0.6
0.4
0.2
0
A
B
A1
B1
0
20
40
60
80
100
120
140
160
180
NUMBER OF STRIPS

Fig.10

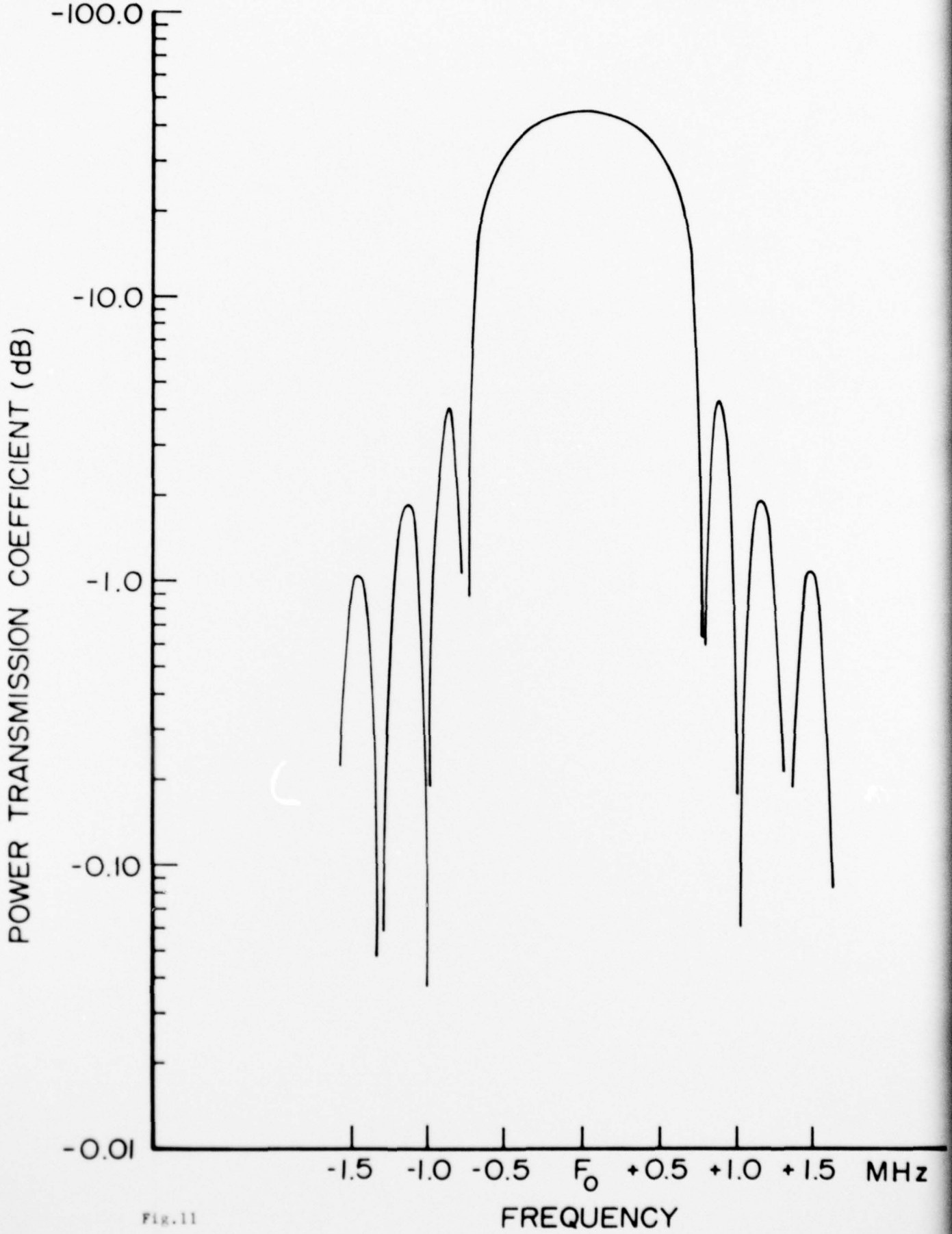
-100.0
-10.0
-1.0
-0.10
-0.01
POWER TRANSMISSION COEFFICIENT (dB)
-1.5
-1.0
-0.5
F0
+0.5
+1.0
+1.5
MHz
FREQUENCY

Fig.11

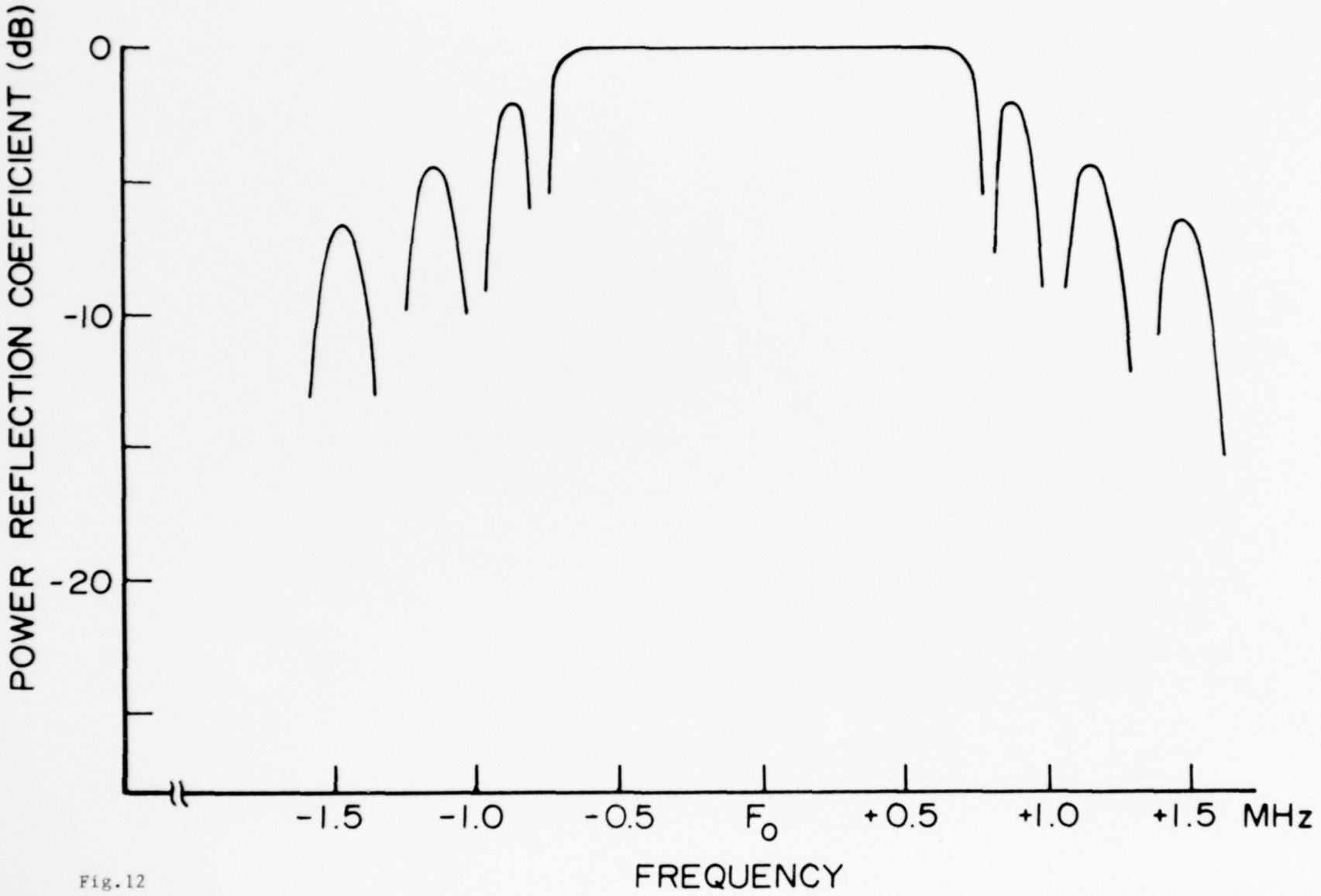
POWER REFLECTION COEFFICIENT (dB)
0
-10
-20
-1.5
-1.0
-0.5
F_0
+0.5
+1.0
+1.5 MHz
FREQUENCY

Fig. 12

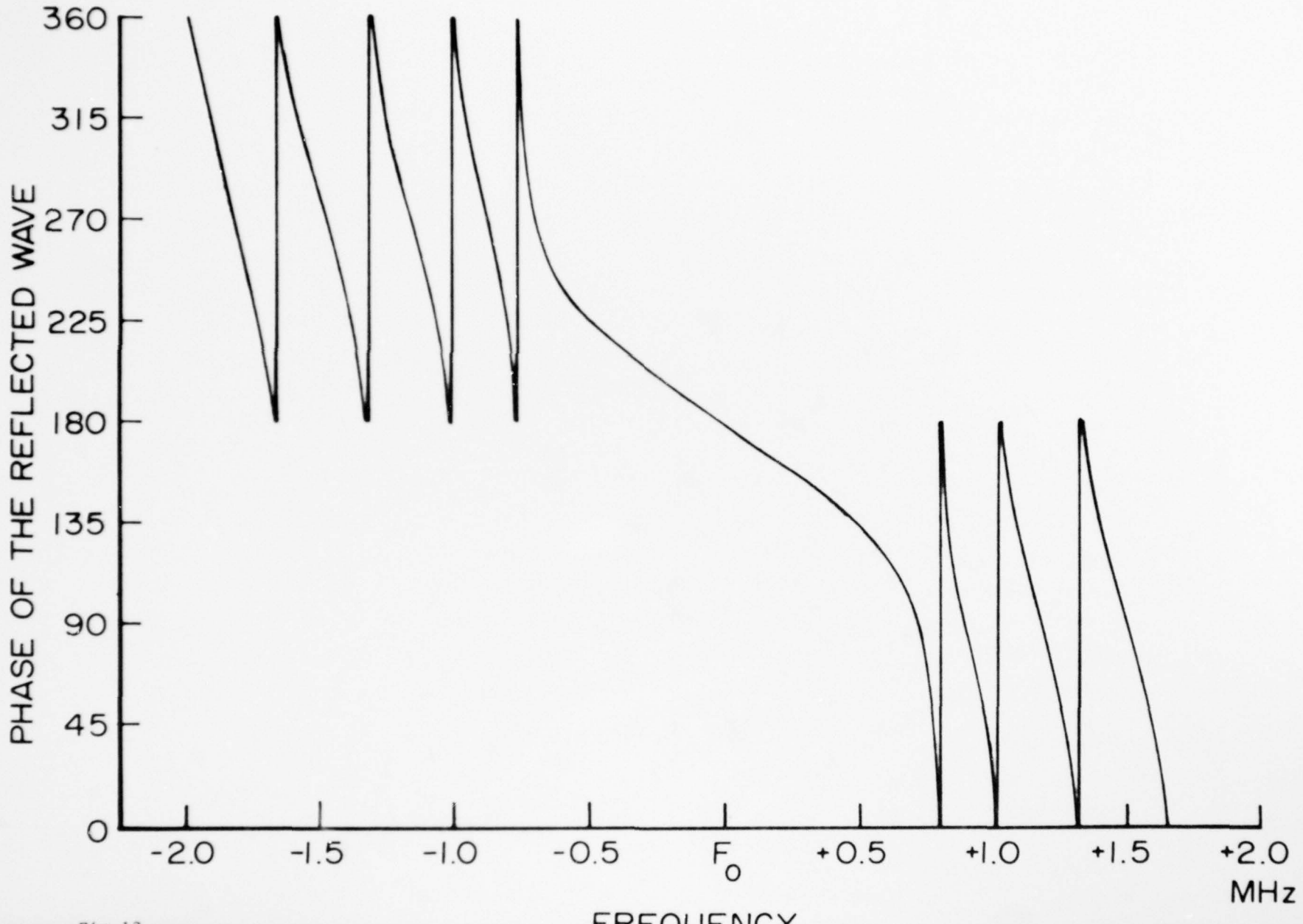
360
315
270
225
180
135
90
45
0
PHASE OF THE REFLECTED WAVE
-2.0
-1.5
-1.0
-0.5
F_o
+0.5
+1.0
+1.5
+2.0
MHz
FREQUENCY

Fig.13